

Using two-way nesting technique AGRIF with MARS3D V11.2 to improve hydrodynamics and estimate environmental indicators

Sébastien Petton¹, Valérie Garnier², Matthieu Caillaud³, Laurent Debreu⁴, Franck Dumas⁵

¹Ifremer, Univ Brest, CNRS, IRD, LEMAR, 11 Presqu'île du Vivier, F-29840 Argenton, France

5 ²Ifremer, Univ Brest, CNRS, IRD, LOPS, 1625 Route de Sainte-Anne, F-29280 Plouzané, France

³Ifremer, DYNECO, 1625 Route de Sainte-Anne, F-29280 Plouzané, France

⁴INRIA, Univ Grenoble Alpes, CNRS, LJK, F-38000 Grenoble, France

⁵SHOM / STM / REC, 13 Rue de Châtellier CS 92803, 29228 Brest CEDEX 2, France

10 *Correspondence to:* Sébastien Petton (sebastien.petton@ifremer.fr)

Abstract. In the ocean, meso / submesoscale structures and coastal processes are associated with fine scales. The simulation of such features thus requires the hydrodynamic equations to be solved at high-resolution (from a few hundred meters down to a few tens of meters). Therefore, local mesh refinement is a primary issue for regional and coastal modelling. AGRIF (Adaptive Grid Refinement In Fortran) library is committed to ~~ackling such a challenge for structured grids~~. It has been implemented in MARS3D, ~~a semi-implicit free surface~~ numerical model developed by Ifremer (the French Research Institute for Exploitation of the Sea) for coastal environmental ~~research~~ and studies. ~~As its time scheme uses an Alternate Direction Implicit (ADI) algorithm, the two-way nesting implementation differs from the one in explicit models~~. The present paper describes ~~the specifics of the AGRIF introduction and~~ how the ~~nesting~~ preserves some essential properties (mass, momentum ~~and tracer~~ conservations) along with the induced constraints (~~bathymetric coherence between grids~~, increase in computation cost). The use and the performance of this new tool are detailed over two configurations that illustrate the wide range of scales and resolutions typically targeted by coastal applications. The first one is based on multiple high-resolution (500m) grids that pave the coastal ocean over thousands of ~~kilometers~~, allowing a continuum between the regional and coastal scales. The second application is more local and has a finer resolution (50m). It targets a recurrent question for semi-enclosed bays: the renewal time indicator. Throughout these configurations, the paper intends to compare the two-way nesting method with the traditional 25 one-way approach. ~~It highlights how the MARS3D-AGRIF tool proves to be an efficient way to~~ ~~both~~ improve the physical hydrodynamics and unravel ecological challenges.

1. Introduction

In the ocean, many observations have clearly shown that turbulence is ubiquitous and that flows are turbulent at all scales (~~Capet, 2015~~). It is also admitted that capturing the whole range of oceanic scales is far beyond the capabilities of any numerical 30 model for a long time to come. ~~Indeed~~ Large Eddy Simulation (LES) approach dedicated to ~~solving~~ the direct forward turbulent energy cascade is far from being reachable except for strict localized places. Therefore, it is necessary ~~to~~ develop relevant and

a supprimé: As over structured grids,

a supprimé: tackle this

a supprimé: .

a supprimé: which is a

a supprimé: researches

a supprimé: dedicated implementation

a supprimé: and

a supprimé: need of

a supprimé: kilometres

a supprimé: and

a supprimé: significantly

a mis en forme : Anglais (E.U.)

a mis en forme : Anglais (E.U.)

a supprimé: Even

a supprimé: solve

a supprimé: not only

efficient parametrizations at subgrid scale and propose refinement capabilities in ocean models to focus the computational grid at key locations. A key region can vary considerably based on geographic or dynamical considerations. As the circulation is obviously tightly controlled by the coastline and more generally by the bathymetry, increasing the resolution of the grid may be essential to properly catch the coastal morphology (e.g., estuaries, cape, peninsulas, small bays and lagoons...).

50 Alternatively, a key region may be where critical processes take place and determine the circulation or fate of a coastal discharge, even far offshore. The Strait of Gibraltar, where internal jumps and consequently internal solitary wave trains are generated, is a perfect illustration, as these features propagate for hundreds of kilometers (Naranjo et al., 2014) until they break and reinforce mixing. Thus, the generating area must be addressed with both sufficient resolution and even locally adapted physics (here non-hydrostatic) to reproduce such structures. Then they must be accurately propagated, possibly outside the refined area.

55 Multiple strategies can be investigated (and are available with some degree of efficiency and accuracy) to tackle the spatial refinement in limited areas. A first one relies on unstructured grids together with finite volume or finite element discretizations: numerous models such as Delft-3D (Roelvink and van Banning, 1995), SLIM (Delandmeter et al., 2018), TELEMAC-3D (Janin et al., 1993) or T-UGOm (Piton et al., 2020) have shown for years their capability to cope with complex geometrical

60 features such as river deltas or continental slope. A second one is based on curvilinear either orthogonal (Rétif et al., 2014; Diaz et al., 2020; Marsaleix et al., 2006; among many others) or non-orthogonal (Grasso et al., 2018) grids. However, the design of such grids might be a great deal of work with a lack of flexibility.

These approaches have also raised the classical issues related to continuously adaptive subgrid parametrization: how to manage both temporal and spatial refinements so that computational cost required by the finest grid cells does not spill over to the entire grid? Recently (Li, 2021) proposed a 2D shallow water mode discretized on a regional spherical multiple-cell which circumvents this constraint. An alternative method applies to structured grids and provides a refinement capability (adaptive or not) to recursively integrate a hierarchy of grids at different resolutions. This kind of approach was proposed in the early eighties (Berger and Olinger, 1984) and has already been implemented in either academic works (Penven et al., 2006; Debreu et al., 2012) or for large-scale realistic applications (Biaستoch et al., 2009; Marchesiello et al., 2011) to improve the resolution

70 and hence the realism of the local dynamics.

Such an approach, the Adaptive Grid Refinement In Fortran (AGRIF) (Debreu et al., 2008), is based on domain decomposition and needs partial overlapping of same level grids. It is expected to facilitate the offshore continuum for coastal applications, despite the overlapping constraint. Therefore, the AGRIF software has been introduced into MARS3D (Lazure and Dumas, 2008), a numerical model dedicated to coastal environmental applications. The main challenge was related to the semi-implicit

75 time scheme. The two-way nesting is now fully operational for mass, momentum and tracer conservation. Implemented along the coasts of the north western European shelf and over coastal bays, the mesh refinement should allow the representation of a large spectrum of spatial (small bays and large areas) and temporal (fast as tides or surges and slow as mesoscale or frontal instabilities) scales.

a supprimé: the ...ubgrid scale, but also to...and propose refinement capabilities in ocean models in order...to focus the computational grid at key locations. A key region can vary considerably based on geographic or dynamical considerations. As the circulation is obviously tightly controlled by the coastline and more generally by the bathymetry, increasing the resolution of the grid may be essential to properly catch the coastal morphology (e.g., estuaries, cape, peninsulas, small bays and lagoons...). Alternatively, a key region may be an area ...here essential...ritical processes take place that shape...nd determine the circulation or a ...ate of a coastal discharge, even far offshore. The Strait of Gibraltar, where internal jump...umps and consequently an ...nternal solitary wave tra (... [1]

a mis en forme (... [2]

a supprimé: SYMPHONIE (Marsaleix et al., 2006),

a mis en forme (... [3]

a mis en forme (... [4]

a mis en forme (... [5]

a mis en forme (... [6]

a mis en forme : Anglais (E.U.)

a supprimé:)

a supprimé: grid. The ...rids. However, the design of such structured curvilinear grid (... [8]

a mis en forme (... [7]

a supprimé: In addition to the need to create efficient tools to manage the grid building, this kind of approach has

a mis en forme (... [9]

a supprimé: integrate

a mis en forme (... [10]

a mis en forme : Anglais (E.U.)

a mis en forme : Anglais (E.U.)

a mis en forme (... [11]

a mis en forme (... [12]

a supprimé: Despite the overlapping constraint, it...t is expected to facilitate the offshore continuum for coastal applications. Consequently...despite the overlapping constraint. Therefore, the AGRIF software has been introduced into a coastal numerical model, namely ... (... [13]

a mis en forme : Anglais (E.U.)

a supprimé: ... a numerical model dedicated to coastal environmental applications. The main challenge was related to the semi-implicit time scheme. The two-way nesting is now fully operational for mass and... momentum and tracer conservation. Implemented along the coasts of the north western European shelf and over coastal bays, the mesh refinement should allow the representation of a large spectrum of spatial (small bays and large areas) and temporal (fast as tides or ...urges and slow as mesoscale or frontal instabilities) scales. (... [14]

a mis en forme : Anglais (E.U.)

This paper aims to demonstrate the capabilities and benefits of the two-way nesting method for modeling the interplay of coastal and regional dynamics. Section 2 describes the recent developments in the hydrodynamic model MARS3D with AGRIF library and addresses the running performance. Afterward, two applications are presented. Sect. 3 depicts a regional model configuration and focuses on the systematic refinement capability. Sect. 4 introduces a focused coastal configuration to highlight two-way nesting improvements. Finally, these results and perspectives are discussed in Sect. 5.

a supprimé: the modelling of...odeling the interplay of coastal and regional dynamics. Section 2 describes the recent developments in the hydrodynamic model MARS3D with AGRIF library,...and addresses the running performance are addressed. Afterwards... Afterward, two applications are presented. In ...ect. 3,...depicts a regional modeled...odel configuration is depicted ...nd focused...ocuses on the systematic refinement capability. In ...ect. 4,... introduces a focus...ocused coastal configuration is introduced to highlight two-way nesting improvements. Finally, these results are are discussed ...nd futures ...erspectives are given ... [15]

2. Innovative developments for two-way nesting

2.1. The MARS3D model (V11.2 released in March 2018)

The hydrodynamic MARS3D (Model for Applications at Regional Scale) model solves the primitive equations under the Boussinesq and hydrostatic assumptions. It uses finite differences over a staggered Arakawa C-grid with a vertical generalized-sigma coordinate framework. It relies on a barotropic/baroclinic mode splitting. The barotropic mode, which obeys the shallow water equation systems, is treated with a modified Alternating Direction Implicit (ADI) algorithm (Leendertse and Gritton, 1971). Unlike split explicit free surface models, the temporal integration of both barotropic and baroclinic modes is carried out with the same time step due to a wider stability range of the barotropic mode. The barotropic/baroclinic coupling is simplified but the propagation of the barotropic mode is weaker as the scheme is implicit. The original time scheme described in Lazure and Dumas (2008) for MARS3D V6 has been significantly modified. First, by adding a prediction step (assessment of depth averaged velocity $v^{n+1,*}$). Second, by alternating the sweep of the computational grid in a row-column-wise manner and then column-row-wise. These modifications have been introduced to limit the spatial split errors inherent to single time step schemes. The row-column-wise form is developed in Eq. (1): it consists in computing (depth averaged velocity u^{n+1} and sea surface elevation $\eta^{n+1,*}$) and then (v^{n+1}, η^{n+1}) in the first half time step. The second half time step, which gives symmetrically firstly $(v^{n+1}, \eta^{n+1,*})$ then (u^{n+1}, η^{n+1}) is not detailed. The first equation of the system is a local solver, whereas the second and the third equations solved together lead to a linear tridiagonal system whose size is twice the number of grid cells in a row because the unknown vector is made of $(u^{n+1}, \eta^{n+1,*})$. Similarly, the fourth and fifth equations lead to a linear tridiagonal system whose size is twice the number of points in a column.

a supprimé: MARS3D V6 is fully described in (Lazure and Dumas, 2008). ...t relies on a mode ...arotropic / ...baroclinic mode splitting. The barotropic mode, which obeys the shallow water equation systems, is treated with a modified Alternating Direction Implicit (ADI) algorithm. Contrary to ... [16]

a supprimé: and due to the wider range of stability of the barotropic mode... the temporal integration of both barotropic and baroclinic modes is carried out with the same time step which on the one hand simplifies the ...ue to a wider stability range of the barotropic mode. The barotropic/baroclinic coupling is simplified but on ...he other hand filters...ropagation of the barotropic mode is weaker as long as ...he numerical filter...cheme is implicit rather explicit. The original ADI algorithm (Leendertse and Gritton, 1971) has been significantly modified by first adding a prediction step (assessment of $v^{n+1,*}$) and then by alternating the sweep of the computational grid in a row-column-wise manner and in a column-row-wise manner. These modifications were introduced to limit the spatial split errors inherent to single time step schemes. The row-column wise manner is developed in Eq. (1): it consists in computing $(u^{n+1}, \eta^{n+1,*})$ in the first step and then (v^{n+1}, η^{n+1}) . The second half time step which gives in a symmetric manner firstly $(v^{n+1}, \eta^{n+1,*})$ then (u^{n+1}, η^{n+1}) is not detailed. ... [17]

a déplacé vers le bas [1]: , $\eta^{n+1,*}$) then

a déplacé vers le bas [2]: , η^{n+1}) is not detailed.

a déplacé vers le bas [3]: . Similarly, the fourth and fifth equations lead to a linear tridiagonal system

a supprimé: $(u^{n+1}$

a supprimé: The first equation of the system is a local solver whereas the second and the third equations solved together lead to a linear tridiagonal system which size is twice the number of grid cells in row because the unknown vector is made of $(u^{n+1}, \eta^{n+1,*})$

a supprimé: which size is twice the number of points in column

a déplacé (et inséré) [1]

a déplacé (et inséré) [2]

a déplacé (et inséré) [3]

a supprimé: $v^{n+1,*} = v^n$

a supprimé: $h^{n+1}...h^{n+1} + \partial\partial y h^{n+1}, *$... [18]

a supprimé: $u^{n+1} =$

a supprimé: $h^{n+1}...h^{n+1} + \partial\partial y h^{n+1}$... [19]

a supprimé: $v^{n+1} =$

$$v^{n+1,*} = v^n - g\Delta t \frac{\partial \eta^n}{\partial y} + \Delta t G_v(u^{n-1}, v^{n-1})$$

$$\eta^{n+1,*} = \eta^n - \Delta t \left[\frac{\partial}{\partial x} (h^n u^{n+1}) + \frac{\partial}{\partial y} (h^n v^{n+1,*}) \right]$$

$$u^{n+1} = u^n - g\Delta t \frac{\partial}{\partial x} (\alpha \eta^n + (1-\alpha) \eta^{n+1,*}) + \Delta t G_u(u^n, v^n)$$

$$\eta^{n+1} = \eta^n - \Delta t \left[\frac{\partial}{\partial x} (h^n u^{n+1}) + \frac{\partial}{\partial y} (h^n v^{n+1}) \right]$$

$$v^{n+1} = v^n - g\Delta t \frac{\partial}{\partial x} (\alpha \eta^n + (1-\alpha) \eta^{n+1}) + \Delta t G_v(u^n, v^n) \quad (1)$$

In the Eq. (1), h stands for the total water depth, Δt is the time step and α is the implicit coefficient of the external pressure gradient term. The term $G_{u/v}(u^n, v^n)$ gathers the vertical average of all the remaining terms including the non-linear and the horizontal dissipation terms, the Coriolis force, and the friction at the surface and the bottom. All of these last ones are explicit and not discussed here.

The linear tridiagonal system is a non-local solver: $\eta^{n+1,*}$ and u^{n+1} are solved over a whole row by the ADI algorithm. Then, for a massive parallel computation, based on a decomposition domain made of horizontal tiles, η^n and u^n are distributed on the different tiles crossed by the considered row (Fig. 1). The linear system can be schematically written as diagonal blocks where each block represents the linear tridiagonal system over a tile:

$$\begin{pmatrix} \text{coef on tile 1} & \cdots & 0 \\ \vdots & \ddots & \vdots \\ 0 & \cdots & \text{coef on tile n} \end{pmatrix} \begin{pmatrix} \eta, u \text{ on tile 1} \\ \vdots \\ \eta, u \text{ on tile n} \end{pmatrix} = \begin{pmatrix} \text{rhs on tile 1} \\ \vdots \\ \text{rhs on tile n} \end{pmatrix} \quad (2)$$

It shows that η and u need to be gathered into a single row tile and that once the linear tridiagonal system is solved, the solution has to be broadcasted back to the original geographic tiles. In order to reduce the communications, the first three equations of the system (1) have been rearranged into the system (3) thanks to the splitting of u^{n+1} into an explicit part and an implicit one.

This leads to a tridiagonal system in which the unknown vector is made solely of $\eta_i^{n+1,*}$:

$$\begin{aligned} v^{n+1,*} &= v^n - g\Delta t \frac{\partial \eta^n}{\partial y} + \Delta t G_v(u^{n-1}, v^{n-1}) \\ u^{n+1,*} &= u^n - g\Delta t \alpha \frac{\partial \eta^n}{\partial x} + \Delta t G_u(u^n, v^n) \\ -g\Delta t^2(1-\alpha) \frac{\partial}{\partial x} \left[h^n \frac{\partial \eta^{n+1,*}}{\partial x} \right] + \eta^{n+1,*} &= \eta^n - \Delta t \left[\frac{\partial}{\partial x} (h^n u^{n+1,*}) + \frac{\partial}{\partial y} (h^n v^{n+1,*}) \right] \\ u^{n+1} &= u^{n+1,*} - g\Delta t(1-\alpha) \frac{\partial \eta^{n+1,*}}{\partial x} \end{aligned} \quad (3)$$

As a result, the length of the ADI system is now precisely the number of grid cells in the x -direction for a given row, and the data involved in the message passing interface between tiles is reduced by a factor of 2. The same methodology is applied to the fourth and fifth of system (1) in the y -direction.

In addition to the modification of the barotropic solver itself, some additional modifications have been implemented in the barotropic/baroclinic coupling because the original iterative coupling described by Lazure and Dumas (2008) was not compatible anymore with the reformulation (3). The coupling that can be sketched according to Fig. 2 is now straightforward:

(a) the barotropic mode being forced with vertically integrated terms of advection, horizontal dissipation, Coriolis, internal pressure gradient and the bottom friction (assessed with the first level of velocity); (b) the baroclinic mode being forced with the external pressure gradient; (c) the last classical step of the coupling consists in redistributing the vertical mismatch between the barotropic transport and the vertically integrated baroclinic transport in order to ensure mass conservation.

Last but not least, the wet-drying capability has been modified to introduce partial drying or wetting. It consists in introducing to the non-local continuity equation a coefficient f_{wet} that evolves in time according to Eq. (4):

a supprimé: In ... the linear tridiagonal system is a context ... [20]

a supprimé: these equations are solved using a ... based on a decomposition domain into ... ade of horizontal tiles. The main drawback of the ADI is its non-local solver for a given row (second and third gathered equations of Eq. (1)) which elements ... [21]

a supprimé: various ... ifferent tiles crossed by the row considered. The solver consists of a linear system which coefficients are distributed on various tiles ... row (Fig. 1). The linear system associated to Fig. 1 ... an be schematically written as diagonal blocks linear system ... here each block is itself ... [22]

a supprimé: clearly raised the question of gathering

a supprimé: on a single tile to solve it and the broadcast ... s solved, the solution (vector made of the (u, η) for the whole row) from the single tile used for the solver ... [23]

a supprimé: each appropriate ... e broadcasted back to the original geographic tile. It induces a wide set of MPI messages commensurable with twice the size of the row ... tiles. In order to by a factor of two ... he communications, the first three equations of system (1) were ... [24]

a supprimé: which unknown vector is made solely of $\eta_i^{n+1,*}$. Therefore, for a given row j , the size is exactly the number of grid cells in the x -direction instead of twice this size for the regular ADI algorithm for which unknown vectors are made of $\eta_i^{n+1,*}$ and u_i^{n+1} . Thus, it reduces the size of the data involved in the message passing interface between tiles by a factor of 2.

a supprimé: $v^{n+1,*}$

a supprimé: v^n

a supprimé: $u^{n+1,*} = u^n$

a supprimé: $-g\Delta t^2(1-\alpha) \frac{\partial}{\partial x} u^{n+1} = u^n$

a supprimé: were performed ... ave been implemented in the barotropic/baroclinic coupling. The ... [25]

a supprimé: (

a supprimé: ,

a supprimé: which was designed for the Eq. (1) has been abandoned as it ... was not compatible anymore with the reformulation (3). The coupling that can be sketched according to Fig. 2 is not iterative anymore to get a convergence of the coupling terms. It is now straightforward: (a) the barotropic mode being forced with vertically integrated terms of advection, horizontal dissipation, Coriolis, internal pressure gradient and the bottom friction (assessed with the first level of horizontal ... elocity); (b) the baroclinic mode is ... eing forced with the external pressure gradient; (c) The ... he last classical step of the coupling consists in redistributing the ve ... [27]

a mis en forme : Anglais (E.U.)

a mis en forme ... [26]

a supprimé: and flooding ... apability has been modified in order to introduce partially ... artial drying or wetting. It consists in ... [28]

a supprimé: for partially dried cells into

$$\eta^{n+1} S f_{wet}^{n+1} = \eta^n S f_{wet}^n - \Delta t [\partial_x(\bar{h}^n u^{n+1}) \Delta y + \partial_y(\bar{h}^n v^{n+1}) \Delta x] \quad (4)$$

where S stands for the grid cell surface ($S = \Delta x \Delta y$) and f_{wet} is the time-dependent fraction of the grid cell that is flooded ($0 \leq f_{wet,i,j} \leq 1$). f_{wet} is given by a prognostic equation accounting for the bottom slope within the grid cell and the water column height at its center.

2.2. The AGRIF library: Mesh refinement and grid interactions

AGRIF (Adaptive Grid Refinement In Fortran from Debreu et al., 2008) is a package for the integration of Structured Adaptive Mesh Refinement (SAMR) features within a multidimensional finite difference model. Its main objective is to simplify the integration of SAMR functionalities within an existing model, while making minimal changes. In particular, it includes a lexicographic analyzer of Fortran code that generates, at the compilation step, the data structures required for running the same code on any grid hierarchy. AGRIF is currently used in the following ocean models: ROMS-AGRIF (Debreu et al., 2012; Penven et al., 2006), a regional model developed jointly at Rutgers and UCLA universities; NEMO ocean modeling system (Biaostoch et al., 2018, 2009), a general circulation model used by the European scientific and operational communities; and HYCOM a regional model developed jointly by the University of Miami and the French Navy. In MARS3D, a one-way nesting implementation ensuring only mass conservation (Muller et al., 2009) was first introduced, followed by a two-way nesting for temperature and salinity only (Dufois et al., 2014). This paper aims to introduce a comprehensive two-way nesting in accordance with the improved MARS3D time scheme, along with its evaluation in coastal environments.

2.2.1. General algorithm

For a general review of two-way nesting algorithms, the reader is referred to Debreu and Blayo (2008). This section overviews the introduction of AGRIF two-way nesting into MARS3D. The challenge was related to the implicit nature of the MARS3D time scheme, the ADI algorithm and the wet-drying capability. Figure 3 illustrates two child grids covering subdomains ω of the parent domain Ω . Their boundaries are delimited by the interfaces Γ . The coarse resolution grid has a mesh size given by Δx_H , while the fine resolution grid has a mesh size of $\Delta x_h = \Delta x_H / \rho$ where ρ is the spatial mesh refinement ratio (an integer). Subscripts H and h stand for the coarse and refined domains, respectively. The partial differential equations solved by the model can be written in the generic forms:

$$\frac{\partial q_H}{\partial t} = L_H(q_H), \quad \frac{\partial q_h}{\partial t} = L_h(q_h) \quad (5)$$

L_H and L_h represent the same continuous operator L at the coarse (H) and fine (h) resolutions. On the child grid, equations are integrated from an initial state, which refers to the conservative spatial interpolation of the initial condition on the coarse grid. Throughout the time integration, the child grid lateral boundary conditions at the interface Γ are provided by temporal and spatial conservative interpolations from the coarse grid. In two-way mode, the coarse solution is updated using the fine solution once the temporal integration of the fine grids is completed, that is, after ρ , sub-time steps. In short, this nesting uses two

a supprimé: $\eta^{n+1} S f_{wet}^{n+1}$

a supprimé: which

a supprimé: centre

a supprimé: (

a supprimé: (...) is a package for the integration of Structured Adaptive Mesh Refinement (SAMR) features within a multidimensional finite difference model. Its main objective is to simplify the integration of SAMR functionalities within an existing model, whilst...hile making minimal changes. In particular, it includes a lexicographic analyser (... [29])

a mis en forme : Anglais (E.U.)

a mis en forme : Anglais (E.U.)

a supprimé: modelling

a mis en forme : Anglais (E.U.)

a mis en forme

(... [30])

a supprimé: For...n MARS3D model... a first...ne-way nesting implementation was introduced to assure the...nsuring only mass conservation with one-way nesting (... [31])

a supprimé: and in...as first introduced, followed by a two-way nesting only (... [33])

a mis en forme

(... [32])

a supprimé: The...his paper aims to introduce a comprehensive two-ways...ay nesting is now fully operational for mass and momentum conservation taking into account intertidal areas (... [35])

a mis en forme

(... [34])

a supprimé: (

a supprimé: ,

a mis en forme : Anglais (E.U.)

a mis en forme

(... [36])

a supprimé: general algorithm introduced in...ntroduction of AGRIF two-way nesting into MARS3D characterized as a split... The challenge was related to the implicit free surface model (... [37])

a supprimé: and their

a supprimé: it is...n integer). Subscripts H and h stand respectively...or the coarse and the...efined domains... respectively. The partial differential equations solved by the model are...an be written in the following...eneric form (... [38])

a supprimé:

They are integrated from an initial state and with lateral open boundary conditions prescribed at the limits of Ω . These equations are discretized on the coarse (H) and fine (h) grid domains by: $\frac{\partial q_H}{\partial t} = L_H(q_H)$

Thus

a supprimé: are the discretizations of

a supprimé: different...he coarse (H) and fine (h) resolutions. The...n the child grid, equations are integrated from an initial state, which refers to the conservative spatial interpolation of the tr (... [39])

different operators: a spatio-temporal interpolator (P) and a restriction operator (R) respectively. Using an explicit convention to simplify, the algorithm can be written in the following conceptual form for a single coarse grid half time step:

a supprimé: Assuming that the model is fully
a supprimé: time step of the

- 565 (1) $q_H^{n+1} = L_H(q_H^n)$ (Temporal integration of the coarse grid)
 (2) For $m = 1 \dots \rho_t$ Do

$$q_h^{n+\frac{m}{\rho_t}} \Big|_{\Gamma} = P(q_H^n, q_H^{n+1})$$
 (Computation of Open Boundary Conditions from the coarse grid to the child grid)

$$q_h^{n+\frac{m}{\rho_t}} = L_h \left(q_h^{n+\frac{(m-1)}{\rho_t}} \right)$$
 (Temporal integration of the child grid)
 (3) $q_H^{n+1} |_{\omega} = R(q_h^{n+1})$ (Update of the coarse grid over the area of overlapping) (6)

a supprimé: 7
a supprimé:) which is
a supprimé: if the model is
a supprimé: The step
a supprimé: the
a supprimé: corresponds to

570 Here, ρ_t is the time refinement factor ($\rho_t = \Delta t_H / \Delta t_h$), equal to the space refinement factor ρ for models restricted to a CFL (Courant Friedrichs Levy) stability condition. Step (1) corresponds to the integration of the coarse grid model for one time step Δt_H on Ω , while step (2) is the integration of the fine grid model over ρ_t time steps. The interpolator P makes use of q_H^n and q_H^{n+1} to produce space and time interpolations on the interface Γ . Step (3) is the update procedure in the two-way nesting, applied every half time step of the coarse grid.

575 2.2.2. Open Boundary Conditions

At the boundaries of the subdomains, the mother grid provides the high-resolution grids with the free surface, tracers and barotropic and baroclinic velocity components. These variables need to be interpolated onto the fine grid by combining Piecewise Parabolic Method (in the normal direction to the boundary) and linear method (in the along direction to the boundary) because the first external (i.e., not-computed) fine grid points (u, v or η) used as open boundary conditions do not coincide with any coarse grid point. Afterward, the open boundary operators (characteristics and radiation methods for momentum and tracer, respectively) are applied to force the fine grid. In a sense, the various fluxes entering the fine grid are not the exact same than the ones seen by the coarse grid: the local conservation is not achieved at boundaries but this potential mismatch is limited by the bathymetric coherence between grids. Moreover, the update step ensures the conservation of the global system (see Sect. 2.2.3).

a supprimé: Due to the arrangement of the grids along the Γ interface, these open boundary conditions require bidimensional interpolation as long as the first external (i.e., not-computed) fine grid points (u, v or η) used for open boundary conditions do not coincide with any coarse grid point. These variables are
a supprimé:). Afterwards
a supprimé: (characteristics or
a supprimé: respectively
a supprimé: computed
a supprimé: that
a supprimé: that output from the coarse grid. Thus,
a supprimé: coarse grid plus fine grids) is reached thanks to the update step (
a supprimé: As explained in (Debreu and Blayo, 2008), the sponge layer...
a supprimé:
a supprimé: on

585 In addition, a sponge layer is set along the open boundaries. It is implemented as a diffusion term that acts on the difference between the high-resolution solution and the interpolation (1) of the coarse resolution solution onto the fine grid (Debreu and Blayo, 2008):

$$\frac{\partial q_h}{\partial t} = L_h + \nabla \cdot (\mu \nabla (q_h - I_h^n q_H)) \quad (7)$$

where μ is a coefficient ranging from its maximal value μ_0 at the interface to 0 a few grid points away from it (usually at a distance of 3 coarse grid cells). This sponge layer is applied both on momentum and tracers. It aims at filtering out scales that are not affordable by the coarse grid and to get a better match in terms of scales between the open conditions (coming out from

a supprimé: term

the coarse grid) and the fine grid state variable q_h at first inner points along the boundary, which come out from operator L_h whose spectral range is wider.

a supprimé: open

a supprimé: conditions of the fine grid

a supprimé: the

a supprimé: which

620 2.2.3. Free surface, tracer and velocity updates with wetting and drying

After the time integration of the high-resolution grids, the information is fed back to the parent grid in the two-way context: the updated coarse solution comes from the spatial average of the fine solution over the whole area of overlapping. This constraint is related to the semi-implicit solver used in MARS3D. Therefore, the mother and child bathymetries need to be constructed so that the bathymetry reduction conserves volume. In doing so, the restriction operator (R) keeps the fluxes coherent and conserve mass.

a supprimé: becomes

a supprimé: . In order for this restriction operator (R)

a supprimé: keep the fluxes coherent and conserve mass

a supprimé: have been

a supprimé: Contrary to split explicit models for which a limited updated area next to the boundary of overlapping is required, the semi-implicit solver used in Mars require to update the full area of overlapping as long as the barotropic solver is not local (but across the full domain).

a supprimé: In a free surface ocean model, for

a supprimé: x

a supprimé: y

a supprimé:):

a supprimé: has be

a supprimé: one considers

a supprimé: (and assuming there is no time refinement)

For conservation reasons, the discrete time evolution of the free surface elevation can be written in terms of the divergence of the barotropic transports U and V in the x and y directions (volumetric fluxes) in a free surface ocean model:

$$S_{i,j} f_{wet_{i,j}}^{n+1} \eta_{i,j}^{n+1} = S_{i,j} f_{wet_{i,j}}^n \eta_{i,j}^n - \Delta t \left[U_{i+\frac{1}{2},j} - U_{i-\frac{1}{2},j} + V_{i,j+\frac{1}{2}} - V_{i,j-\frac{1}{2}} \right] \quad (8)$$

A consistent update scheme for free surface and barotropic transport is obtained by applying the restriction operator to the right-hand side of this equation. Hereafter, let's consider the situation represented in Fig. 4 where the mesh refinement coefficient is equal to 3. The free surface restriction operator is a simple average of the 9 fine grid cells using the following area weighted formulae:

$$S_{i_c,j_c} f_{wet_{i_c,j_c}}^{n+1} \eta_{i_c,j_c}^{n+1} = \sum_{\substack{i=j_f-1,j_f+1 \\ j=j_f-1,j_f+1}} S_{i,j} f_{wet_{i,j}}^{n+1} \eta_{i,j}^{n+1} \quad (9)$$

where i_c and j_c are the indices of the cell in the coarse grid and i_f and j_f in the fine grid (see Fig. 4). Using Eq. (9), the time evolution of the updated free surface is given by:

$$S_{i_c,j_c} f_{wet_{i_c,j_c}}^{n+1} \eta_{i_c,j_c}^{n+1} = S_{i_c,j_c} f_{wet_{i_c,j_c}}^n \eta_{i_c,j_c}^n - \Delta t \left[\left(U_{i_f+\frac{3}{2},j_f-1} + U_{i_f+\frac{3}{2},j_f} + U_{i_f+\frac{3}{2},j_f+1} \right) - \left(U_{i_f-\frac{3}{2},j_f-1} + U_{i_f-\frac{3}{2},j_f} + U_{i_f-\frac{3}{2},j_f+1} \right) \right. \\ \left. + \left(V_{i_f-1,j_f+\frac{3}{2}} + V_{i_f,j_f+\frac{3}{2}} + V_{i_f+1,j_f+\frac{3}{2}} \right) - \left(V_{i_f-1,j_f-\frac{3}{2}} + V_{i_f,j_f-\frac{3}{2}} + V_{i_f+1,j_f-\frac{3}{2}} \right) \right] \quad (10)$$

Consistently with the average restriction operator for the free surface, the coarse grid barotropic transports can then be updated by the relations:

$$U_{i_c+\frac{1}{2},j_c} = U_{i_f+\frac{3}{2},j_f-1} + U_{i_f+\frac{3}{2},j_f} + U_{i_f+\frac{3}{2},j_f+1} \\ V_{i_c,j_c+\frac{1}{2}} = V_{i_f-1,j_f+\frac{3}{2}} + V_{i_f,j_f+\frac{3}{2}} + V_{i_f+1,j_f+\frac{3}{2}} \quad (11)$$

This corresponds for U to an injection in the x -direction and an average in the y -direction and reciprocally for V . As time refinement is applied, these fluxes have been summed up over the ρ_t fine grid time steps.

a supprimé: x-

a supprimé: y-

approximately the same number of wet grid cells to each MPI rank and excluding the land-masked part of the domain. The hybrid computation combines MPI (domain decomposition) and OMP (distribution of threads in Fortran loops inside each MPI domain) parallelizations. It has been implemented following the MPI_THREAD_FUNNELED type, where MPI calls are only made outside OMP parallel regions.

For a MARS3D/AGRIF configuration with only one child per nesting level, mother and child grids are resolved sequentially with the same parallelization option. It is thus recommended to work with grids of approximately the same number of cells to facilitate the cores distribution. In the case of multiple child grids at the same nesting level, the user can choose between two possibilities for the time integration of the child grids: sequentially or simultaneously. The first solution consists of a sequential integration of each child grid by the set of cores. The second solution involves a distribution of the MPI cores among all child grids at the beginning of the simulation. The cores can be assigned between all child grids or within multiple groups of child grids. The latter option is favorable when the child grids' sizes differ or when the child grids are much smaller than the mother grid.

2.4. Computational cost

To evaluate the performance of this implementation, several tests were performed with the regional and coastal configurations presented in the following sections with classical offline one-way nesting and two-way nesting. First, the coarser model was run independently over the whole computation period to get information to force the child grid area at hourly frequency. Second, baroclinic currents, temperature and salinity variables were interpolated horizontally and vertically onto the child grid with an external homemade Fortran tool. For the regional configuration composed usually of seven child grids, only the one focused on the Iroise sea (see Fig. 5) was kept for this experiment.

Table 1 summarizes the computational times for MARS3D one-way classical offline nesting and MARS3D/AGRIF two-way nesting. For this experiment, the time integration lasts 45 days. All the simulations were performed on the DATARMOR supercomputer, composed of 396 nodes with 28 cores each (<https://wwz.ifremer.fr/pcdm>). Since the computing performance depends on the load of the machine, the computational cost was evaluated from a pool of repeated experiments (five times). For each configuration, the different models (one-way and two-way) run with the same MPI ranks distribution but from two different parallelization methods: the classic MPI domain decomposition and the hybrid computation (MPI + OMP) mode.

Table 1: Mean computation time given in hours for both modeled configurations for a simulation of 45 days.

Configuration	Mode	Cores	Distribution	Scenario	one-way offline	two-way online
Regional	MPI	56	56 MPI ranks	Hydrodynamic only	12.0	15.0
Coastal	MPI	112	112 MPI ranks	Hydrodynamic only	13.5	18.6
Regional	Hybrid	448	56 MPI ranks with 8 OMP threads each	Hydrodynamic only	2.9	4.3

a supprimé: to each MPI rank ...approximately the same number of wet grid cells to each MPI rank and excluding the land-masked part of the domain. The hybrid computation is based on both...ombines MPI (domain decomposition) and OMP (distribution of threads in Fortran loops inside each MPI domain) parallelization...arallelizations. It has been implemented following the MPI_THREAD_FUNNELED type, where MPI calls are only made outside of

a supprimé: unique ...ARS3D/AGRIF configuration with only one child per level ...esting configuration...level, mother and child grids are resolved sequentially with the same parallelization option. To facilitate the distribution of cores, it...t is thus recommended to work with grids of rather...pproximately the same numbers...umber of mesh...ells to facilitate the cores distribution. In the case of multiple child grids at the same nesting level, the user can choose between two possibilities for the time integration of the child grids: sequentially or simultaneously. The first solution consists in...f a sequential integration with the same number of processors for ...f each child grid,...y the set of cores. The second solution involves a distribution of the MPI ranks...ores among all child grids. For this latter, the ranks are allocated to the child grids...at the beginning of simulation, based on the number of wetting cells in every child grid. In this way, ranks... The cores can be assigned between all child or within multiple groups of child grids on the same hierarchical level. This last... The latter option is favorable when the size of grids differs from one another

a supprimé: two different...he regional and coastal configurations presented in next...he following sections with classical offline one-way nesting ang...nd two-way nesting. First, the coarser model has been...as run independently over the whole computation period to get information to force the child grid area at hourly frequency. Baroclinic...econd, baroclinic currents, temperature and salinity variables are then...ere interpolated horizontally and vertically onto the child grid with an external homemade Fortran tool. For the regional configuration composed normally...sually of seven child grids, only the one focused on the Iroise sea (see Fig. 5) was kept for the purpose of

a supprimé: The ...able 1 summarizes the computational times for the simulation of 45 days are provided in the Table 1 for both for both ...ARS3D one-way classical offline nesting or...nd MARS3D/AGRIF two-way nesting. For this experiment, the time integration lasts 45 days. All the simulations have been...ere performed on the DATARMOR supercomputer DATARMOR infrastructure... composed of 396 nodes with 28 cores each (<https://wwz.ifremer.fr/pcdm>). Since the computing performance depends on the load of the machine, the computational cost has been...as evaluated from a pool of repeated experiments (five times). For each configuration, the different models (one-way and two-way) have been ...un with the same parallelized discretization ...PI ranks distribution but with...rom two different parallelization methods: a...he classic MPI domain decomposition and a...he hybrid computation based on both MPI (domain decomposition) and OMP (distribution of threads in Fortran loops inside each ...MPI domain) parallelization

Coastal	Hybrid	336	48 MPI ranks with 7 OMP threads each	Hydrodynamic & 13 passive tracers	21.1	29.2
---------	--------	-----	--------------------------------------	--------------------------------------	------	------

For both configurations, the computation time is increased by one-third for the AGRIF configuration compared to the classical offline one-way nesting. This difference is explained by two extra steps performed by the AGRIF library, the spatial interpolation to prepare the fine grid boundary conditions and the update process from the fine grid to the coarse one. It is worth noticing that the handling time of 3D output files and the waiting time due to the activity on DATARMOR were not included in the one-way nesting duration. Their introduction would decrease the difference especially if several zooms are implemented.

As shown with the regional example, using hybrid parallelization with 8 times more computational resources than with MPI decreases the total time by 4. The hybrid mode is an efficient way to require more resources without considering the domain decomposition in complex geographic areas. Finally, the advection-diffusion evolution of 13 passive tracers in the coastal configuration is another example where hybrid mode makes it possible to achieve reasonable calculation times.

3. Systematic refinement of the coastal zone: Paving the French Atlantic coast within a regional configuration

3.1. Bay of Biscay configuration

The MARS3D model has already been used to investigate the Bay of Biscay and its extension to the western English Channel (Huret et al., 2013; Lazure et al., 2009). Here, the MARS3D/AGRIF capability is implemented along the North-Western European continental shelf. Figure 5 shows how the AGRIF skill is used to pave the coastline from Spain to Belgium with overlapping grids. Seven 500m-resolution zooms of approximately the same grid size are embedded into a coarser 2.5km resolution grid. 40 generalized σ -layers discretize the vertical axis with a stretching function that induces refinement above 150m depth next to the surface. Even though the space refinement factor is 5, the time refinement is adapted according to the maximum velocity encountered within each grid. It is either 3 (over areas with relatively slow flows) or 5 (in very energetic areas such as the middle of the English Channel). Similarly, the turbulent viscosity coefficient (Laplacian operator) differs between each zoom ranging from 0.5 up to 3 m².s⁻¹. At the surface, Météo France atmospheric forcings drive the dynamics: ARPEGE High Resolution (0.1°, hourly) analysis for the coarser grid and AROME (2.5 km, hourly) analysis for the child grids. The main hydrological runoffs are set in the zooms (96 rivers). They come from different source databases (Spain, English, French and Netherlands). At the open boundaries of the coarse grid, daily temperature and salinity conditions are provided by the MERCATOR PSY2V4 re-analysis. The tidal signal is issued from a larger 2D model (5km resolution) forced by the FES 2014 ocean tide atlas with 14 harmonics constituents (Lyard et al., 2021). The sea level is imposed while a zero gradient condition is applied to normal and tangential currents.

A realistic two-way hindcast has been realized over the period 2010-2019. To demonstrate and characterize AGRIF nesting benefits, a one-way configuration has been run on the Iroise grid over the years 2017-2018 as a reference. These two common

- a supprimé:
- a supprimé: with the constant spatial interpolation
- a supprimé: within
- a supprimé: at each
- a supprimé: time step. The
- a supprimé: which assures the fluxes continuity, covers
- a supprimé: area in
- a supprimé: grid and
- a supprimé: also responsible for this increase. For the one- (... [47])
- a supprimé: DATARMOR load
- a supprimé: have
- a supprimé: been taking into account.
- a supprimé: whole
- a supprimé: a ratio
- a supprimé: This last solution
- a supprimé: having to consider
- a supprimé: The
- a mis en forme (... [48])
- a mis en forme (... [49])
- a supprimé: coast line
- a supprimé: zooms with a
- a supprimé: 500m and roughly
- a supprimé: introduced
- a supprimé: 5 km
- a supprimé: that encompasses all the seven grids. The co (... [50])
- a supprimé: ,
- a supprimé: A
- a supprimé: of 5 is used between each grid level but
- a supprimé: locally. Thus, the time refinement coefficient (... [51])
- a supprimé: rather
- a supprimé: in
- a supprimé: In the same way, the horizontal turbulent clos (... [52])
- a supprimé: which
- a supprimé: Two
- a supprimé: hindcasts have
- a supprimé: several years (
- a supprimé: for the two-way and 2017-2018 for the one-way) to
- a supprimé: . For each hindcast
- a supprimé: spin-up of 3 months
- a supprimé: performed.

years have been selected upon the available datasets for several validation parameters detailed in appendix A. A 3-month spin-up was performed for each hindcast. The forcing and parameterization of the offline one-way hindcast are those used in the two-way configuration apart from the tidal sea level signal, which comes from the 112 harmonic components of the SHOM CST-France model (le Roy and Simon, 2003). The temperature and salinity open boundary conditions come from the above mother grid integrated without child grids. This tidal model has been accurately validated throughout the French tidal gauge network RONIM.

3.2. Hydrodynamic impact over open boundary conditions

The tidal signal (extracted from Iroise 500m grid) is compared to hourly validated data of four tidal gauges available in the studied area. The main statistics are estimated over one year are given in Table 2. The tide modeled with the two-way technique is slightly less precise than with the one-way simulation. It is especially true at the northeastern boundary, at Roscoff, where the RMSE is twice as large. On the opposite at the southern boundary, at Concarneau, the differences are in favor of the two-way nesting.

Table 2: Comparison of sea surface elevation between MARS3D one-way (normal font) and MARS3D/AGRIF two-way (bold font) for the Iroise zoom (500m horizontal resolution) compare to RONIM tidal gauges.

	Roscoff	Le Conquet	Brest	Concarneau
Normalize standard deviation (%)	1.022	1.010	0.988	1.029
	0.969	1.004	0.990	1.024
Root mean square error (cm)	9.3	7.2	10.5	7.9
	18.7	9.4	12.2	6.4
Pearson correlation coefficient (%)	0.999	0.999	0.998	0.998
	0.985	0.993	0.990	0.995

To observe the influence of the tide propagation, the signal modeled by Iroise zoom is compared to the PREVIMER harmonic component atlas. This atlas was built upon a series of barotropic simulations at 250m horizontal resolution and validated with the RONIM network (Pineau-Guillou, 2013). A harmonic decomposition was applied to each hourly time series extracted from the hindcasts covering an entire year. Table 3 compares the wave elevations for the waves M2, S2, O1, K1 at four locations in the Iroise sea. Both models are in fairly good agreement with the reference atlas. The main difference is found for the wave K1 and MARS3D/AGRIF two-way configuration. The wave K1 is over-estimated by 20% on relative difference, but the amplitude itself differs by less than 2 cm.

Table 3: Comparison of wave elevation amplitudes between MARS3D one-way (normal font) and MARS3D/AGRIF two-way (bold font) for the Iroise zoom (500m horizontal resolution). The model amplitudes are given in cm with the relative difference between model and observation in %.

a supprimé: ongoing issue for nesting models relies on open boundary conditions. For the AGRIF configuration, the tidal propagation is performed using sea surface elevation and fluxes interpolation. For the regional Bay of Biscay configuration, the initial tide forcing is imposed at the mother grid's boundary with FES model, composed of 12 tidal harmonic components. A zero gradient condition is applied to currents. To force the child grid in classic one-way nesting, the SHOM CST-France model is normally used as it contains 112 components and a Dirichlet boundary conditions is applied for currents. This tidal model has been accurately validated throughout the French tidal gauge network RONIM. The modelled

a supprimé: from

a supprimé: gauge

a supprimé: the

a supprimé: for the regional Bay of Biscay configuration.

a supprimé: from

a supprimé: techniques

a supprimé: This occurs

a supprimé: north-eastern

a supprimé: favour

a supprimé: .).

a supprimé: nested configuration has been

a supprimé: with the zoom grids.

a supprimé: has been

a supprimé: has been

a supprimé: hindcast with an

a supprimé: output frequency over a period of one

a mis en forme : Anglais (E.U.)

a mis en forme : Anglais (E.U.)

a supprimé: In

a supprimé: , a comparison of

a supprimé: is given

a supprimé: 4 different points distributed

a supprimé: rather

a supprimé: for the K1

a supprimé: where the wave errors are over estimated by 20%,

a supprimé: difference is

	M2	S2	O1	K1
Point 1	201.3 (-3%)	73.4 (-2%)	7.0 (+9%)	7.5 (+9%)
5.27°W - 48.7°N	198.8 (-4%)	74.0 (-1%)	6.0 (-2%)	8.8 (+29%)
Point 2	169.2 (-1%)	63.8 (-1%)	7.0 (+6%)	7.0 (+5%)
5.27°W - 48.48°N	170.3 (-1%)	63.0 (-1%)	6.4 (-1%)	8.4 (+27%)
Point 3	179.1 (-2%)	65.6 (-2%)	7.0 (+9%)	7.0 (+13%)
5.5°W - 48.3°N	180.0 (-2%)	66.51 (-1%)	6.5 (-2%)	8.5 (+36%)
Point 4	192.2 (-2%)	72.1 (-1%)	7.0 (+5%)	7.3 (+5%)
4.7°W - 48.3°N	192.3 (-2%)	72.3 (-1%)	6.0 (-6%)	8.4 (+21%)

1025

A similar comparison has also been done for the barotropic currents. The differences are higher for the minor waves O1 and K1. They reach up to 5 cm.s⁻¹ and 30% in relative difference at some locations (not shown). However, the validation of the PREVIMER atlas currents was not available all over the area due to a lack of long time series data over the French coast. Barotropic currents have therefore been compared to different available ADCP datasets recorded in the Bay of Brest or Molène archipelago over shallow waters. No significant difference has been found between nesting techniques.

030

3.3. Hydrologic validation

A detailed qualification of the regional Bay of Biscay configuration has been done by Bezaud and Pineau-Guillou (2015). It highlighted the enhancements in predictions with increasing resolution in the coastal areas where the 500m zoom models have been implemented. These comparisons have been made against coarser models. As expected, the authors concluded that a finer resolution allows the model to simulate the small-scale structures (instabilities of the front, eddies, filaments, ...) accurately. Here, the two-way versus one-way nesting is evaluated over 2017-2018. The evaluation focuses on the Iroise Sea zoom with different mooring stations (see black points in Fig. 5 and Fig. 8). Figure 6 displays Taylor diagrams for temperature and salinity. A third diagram represents bias values and root mean squared errors (RMSE). These graphs summarize the comparisons between the available datasets (see appendix A) and both nesting methods.

035

The nesting impact is not homogenous all over the domain. First, the two-way nesting technique improves the model's overall performance compared to oceanic datasets (see green points for one-way and yellow points for two-way). The simulated temperature offsets are noticeably reduced. The primary favorable impact is the drop of the root mean square error by 0.4°C for the COAST-HF MAREL Iroise point. For salinity comparisons, the RMSE and the bias are of the same order of magnitude. The significant improvement relies on the enhancement of correlation for the COAST-HF ASTAN dataset. This could be due to the vicinity of this point to the eastern border of the zoom. The update capability of AGRIF two-way enables more realistic incoming fluxes at high temporal resolution. The relative standard deviation of the simulated salinity at MAREL Iroise buoy is also considerably reduced.

040

045

- a supprimé: This
- a supprimé: also
- a supprimé: between both models
- a supprimé: with difference of
- a supprimé: of 30% for
- a supprimé: points.
- a supprimé: In the same idea, barotropic
- a supprimé: that were
- a supprimé: in
- a supprimé: . As they are mainly situated
- a supprimé: , there have been no
- a supprimé: (
- a supprimé: ,
- a mis en forme : Anglais (E.U.)
- a mis en forme : Anglais (E.U.)
- a mis en forme : Anglais (E.U.)
- a supprimé: has
- a supprimé: of
- a supprimé: and
- a supprimé: conclusions may therefore seem obvious. Indeed,
- a supprimé: accurately
- a supprimé: ...).
- a supprimé: an evaluation of
- a supprimé: nesting
- a supprimé: at the same horizontal scale
- a supprimé: performed
- a supprimé: a two-year period from
- a supprimé: to 2019
- a supprimé: a
- a supprimé: diagram
- a supprimé: (Fig. 6a) or
- a supprimé: (Fig. 6b) and another diagram that
- a supprimé: It appears that the nesting impact is not homogenous over the whole domain.
- a supprimé: of the model
- a supprimé: main favourable
- a supprimé: exhibit to be in
- a supprimé: major
- a supprimé: ability
- a supprimé: As this point is located in the strait of Brest, (... [53])

3.4. Focus on particular processes

In the Iroise Sea during the summer, the Ushant front is depicted by cold water of about 14°C. Over shallow depths, the tidal currents are intensified and very strong around Ushant and Molène archipelago. The induced tidal stirring is so large that waters are mixed (and homogeneous) from the sea surface to the bottom. Further offshore, the summer stratification can develop, and the sea surface is warmer (above 18°C). This phenomenon can be seen from satellite data on 15 August 2016 (Fig. 7) for both Landsat 8 and ODYSSEA products described in appendix A. Compared to ODYSSEA, the Landsat surface temperature is overestimated in different spots near the coast, in the bay of Brest for example, with values over 20°C which might be due to mis-flagged clouds.

The ability of the two-way nesting approach (Fig. 7d) to correctly reproduce this spatial feature is evident while the one-way nesting (Fig. 7c) struggles to simulate this phenomenon. Indeed, the Ushant front is nearly missing in the one-way simulation. It is much better characterized in the two-way simulation at 5.25°W, with more realistic temperature magnitudes on each side of the front, thanks to the AGRIF update. Furthermore, the realism of the sub-mesoscale structures around the shoals of Sein Island and in the Molène archipelago is improved. On the other hand, one can notice the open boundary effect in the south part of the one-way simulation, where an east-west temperature front is created. It is related to the upwind scheme applied to temperature and salinity open boundary conditions (i.e., apply external value when the water mass enters the domain).

For wide open areas such as the Iroise Sea, the benefit of the feedback/update of the zoom contributes to the correct representation of the thermic Ushant front mainly by enlarging the span of scale captured (e.g., fine eddies and filaments), which is expected, but also in terms of the horizontal localization of thermal front, which is less expected. As a matter of fact, the forcing through the open boundaries is of primary importance for limited area models; it may dramatically impact the local coastal processes, even in areas where the dynamics are highly controlled by large scales such as the tidal forcing. Even though the tidal signal is better represented with the one-way nesting (due to the CST-France model), the upwind scheme applied for tracers at open boundaries is not accurate enough for hourly heat exchanges. The chosen simulated domain is not large enough for one-way nesting to reproduce a sharp temperature front.

4. Highlighting the benefit of a two-way conservative approach: Estimating renewal time over a coastal area

4.1 Bay of Brest configuration

The Bay of Brest is a semi-enclosed macro-tidal ecosystem located at the western end of Brittany (France), covering more than 180 km². It is connected to the Iroise Sea through a 1.8-km wide by 6-km long and roughly 50-m deep inlet (called the Goulet de Brest). Due to its complex geometry and topography, the currents are strong but relatively well known, being the purpose of many previous studies. A dominant semi-diurnal tide characterizes this area with a tidal range of 1.2 to 7.3 m. The tidal currents peak up to 3 m s⁻¹ in the Goulet and are in quadrature phase relative to the surface elevation (Petton et al., 2020). The mean volume at mid-tide inside the bay is roughly 2 billion m³. As its average depth is only 8 m, the back-and-forth flow

a supprimé: clearly

a supprimé: on

a supprimé: Fig. 7 for the

a supprimé: of

a supprimé: (Fig. 7a)

a supprimé: (Fig. 7b)

a supprimé: Compare

a supprimé:

a supprimé: clear

a supprimé: and

a supprimé: The

a supprimé: are strengthened

a supprimé: this improvement supports

a supprimé: fine

a supprimé: in

a supprimé: two-way simulation. On another

a supprimé: could

a supprimé: An

a supprimé: is prescribed

a supprimé: when using one-way nesting

a supprimé:

a supprimé: term

a supprimé: horizontal localisation

a supprimé: is

a supprimé: if

a supprimé: sufficient

a supprimé: the

a supprimé: exchange at an hour frequency.

a supprimé: with

a supprimé: get

a supprimé:

a supprimé: macrotidal

a supprimé: is

a supprimé: spanning over

a supprimé: The strong hydrodynamic currents due

a supprimé: This macro-tidal coastal area is characterised by a

a mis en forme : Anglais (E.U.)

a mis en forme : Anglais (E.U.)

a supprimé: of

at each tide prevents stratification nearly everywhere (Le Pape and Menesguen, 1997). The tidal prism is 25% of the mean volume in neap tide and 60% in spring tide. Freshwater runoffs, mainly coming from the Aulne river, modify the hydrology locally (Auffret, 1983).

The MARS3D/AGRIF model has been set up over the Iroise sea (47.74°N - 48.82°N; 4.08°W - 5.55°W) with a horizontal grid resolution of 250m. As shown in Fig. 8, a zoom over the Bay of Brest (48.20°N - 48.44°N; 4.09°W - 4.72°W) is introduced with a resolution of 50m. The time and space refinement factors are both equal to 5. The vertical discretization is performed with 20 equidistant σ -layers in both grids. The bathymetries have been interpolated from a combination of digital terrain models (SHOM, Ifremer, IGN). This Iroise model is forced by harmonic components from the SHOM CST-France atlas (le Roy and Simon, 2003). The 3D open boundary conditions for baroclinic currents, temperature and salinity are imposed at an hourly frequency from a hindcast of the previous regional configuration (Caillaud et al., 2016). Freshwater inputs for the four main rivers in the Bay have been taken from the French HYDRO database (<http://www.hydro.eaufrance.fr/>) and corrected with corresponding watershed surface rates. The atmospheric forcings rely on the Météo France AROME (2.5 km, hourly) analysis. The configuration is available from Petton and Dumas (2022) along with a detailed description of physical and numerical parameterizations.

4.2. Hydrologic validation

Two realistic hindcasts have been run from 2017, to 2019 for both one-way and two-way nesting techniques. Previous studies have already validated the coastal Bay of Brest one-way configuration in detail (Petton et al., 2020; Frère et al., 2017). In fact, the large-scale features of the macro-tidal flow are easily captured (Petton et al., 2020) in such a semi-enclosed area. And due to high turbulent mixing in the area, the dynamics are less sensitive to boundary effects. Consequently, the two-way nesting technique barely enhances the results. The tidal features are the same (not shown), while the hydrology is slightly modified (blue/red points for one-way and two-way, respectively, in Fig. 6). Indeed, the two-way nesting reduces the bias in temperature. The feedback, which enables a more accurate global temperature budget in the mother grid, could explain this improvement. Moreover, the two-way technique reduces the relative standard deviation in salinity for the MAREL Iroise and ECOSCOPA datasets. As the water runoffs are identical, this amelioration might be hard to explain. Nevertheless, it may result in a better simulation of current flows according to nonlinear effects.

4.3. Timescale indicator

As the shallow ocean is subject to considerable environmental and anthropogenic pressures, the fate of coastal waters is a key to environmental, ecological and economic issues. Therefore, global and local indicators are crucial for stakeholders to anticipate the spread of different materials such as oil (Jordi et al., 2006), micro-plastics (Frère et al., 2017), biogeochemical processes due to nutrients release (Le Pape and Menesguen, 1997; Fiandrino et al., 2017), and pollution phenomena (Jiang et al., 2017; Neal, 1966) and to develop restoration solutions (Kininmonth et al., 2010; Rossi et al., 2014; Thomas et al., 2014).

a mis en forme (... [54])

a supprimé: The hydrology is dominated by freshwater... freshwater runoffs, mainly coming mostly (... [55])

a supprimé: The atmospheric forcings rely on the Météo France AROME (2.5 km) analysis with hourly data

a mis en forme (... [56])

a supprimé: is... as been set up over the Iroise sea (geographic limits ... 7.74°N - 48.82°N and... 4.08°W - 5.55°W) with a horizontal grid resolution of 250m. A ... s shown in Fig. 8, a zoom over the Bay of Brest (48.20°N - 48.44°N; 4.09°W - 4.72°W) is introduced with a resolution of 50m (geographic limits 48.20°N - 48.44°N and 4.09°W - 4.72°W), see Fig. 8. (... [57])

a supprimé: are... ave been interpolated from a combination of different ... igital terrain models (SHOM, Ifremer, IGN). The... his Iroise model is forced by harmonic components from the SHOM CST-France model (... [58])

a mis en forme : Anglais (E.U.)

a mis en forme : Anglais (E.U.)

a supprimé: (Inter annual hydrodynamic hindcast with MARS3D-AGRIF model - Bay of biscay and Manche Areas)

a mis en forme : Anglais (E.U.)

a supprimé: more ... etailed description of physical,... and numerical and parallelisation parametrisations from (Petton and Dumas, 2022) (... [59])

a mis en forme : Couleur de police : Noir

a supprimé: realized over... un from 2017 up... to 2019 for both one-way and two-way nesting techniques. The... revious studies have already validated the coastal Bay of Brest one-way configuration has already been validated ... n detail in previous studies (... [60])

a supprimé: The two-way nesting has the same ability to reproduce... n fact, the main characteristics of currents and w (... [62])

a mis en forme (... [61])

a supprimé: this... uch a semi-enclosed area. Its relatively (... [64])

a mis en forme (... [63])

a mis en forme : Anglais (G.B.)

a supprimé: 2

a supprimé: large... onsiderable environmental and anthro (... [65])

a supprimé: or

a mis en forme (... [66])

a mis en forme (... [67])

a supprimé: flushing

a mis en forme (... [68])

a mis en forme : Anglais (E.U.)

a supprimé: or

a mis en forme : Anglais (E.U.)

a mis en forme (... [69])

4.3.1. e-folding flushing time estimate

In this study, the water renewal time in the Bay of Brest is evaluated from the flushing time indicator. This diagnostic gives the time for 67% ($1 - 1/e$) of the water in a control volume to be renewed. As the incoming flow may take some time to reach (parts of) the control volume, the flushing lag t_0 represents the time required for 5% of the water mass to be flushed out by the inflow. It allows understanding where the inflow comes from. Consequently, the e-folding flushing time θ is more precisely the decay time in concentration from 95% down to $1/e$ of initial concentration using an exponential regression $C(t - t_0) = e^{-(t-t_0)/\theta}$ (Jouan et al., 2006; Grifoll et al., 2013; Plus et al., 2009). The e-folding flushing time is estimated locally to provide spatially distributed information on the water renewal capacity of a basin or over the entire control volume. Then the global flushing time is the average of the local flushing times.

In the Bay of Brest, the water inflow can come from the rivers or tidal progression. To identify the relative importance of these two processes, the volume control has to extend over the entire bay plus the outer part of the bay in which only the tide is at play (see dash blue line in Fig. 8). For an accurate estimate of the e-folding flushing time, the simulated domain has to be larger than the control volume (Viero and Defina, 2016). Indeed, the return flow through the Goulet due to the semi-diurnal tide is likely to influence the water mass displacement and therefore the renewal time. Thus, the two-way nesting is expected to be an adequate tool: after crossing the open boundary, a particle can re-enter the simulated domain in the full nesting while it is lost in the one-way method.

In our experiment, the flushing time is estimated on an Eulerian reference system by simulating the dilution of passive tracers whose initial concentration is set to 1 inside the control volume (in the fine grid) and 0 everywhere else. Water coming from the ocean (outside the Iroise sea) and the river's runoffs has a tracer concentration equal to 0. The outflow concentrations are lost when crossing the model grid (mother grid in two-way nesting). To get rid of the initial tide conditions, the release of tracers is repeated 13 times, every hour for an even coverage of the tidal cycle (Plus et al., 2009). The final indicator is the average of the 13 estimations.

4.3.2. Case scenario

Various numerical experiments have been performed to catch variable conditions and estimate an exhaustive renewal indicator. Each simulation has been carried out according to the same protocol, with a hydrodynamic spin-up run performed over one month before the release of passive tracers. To obtain various tidal regimes and hydrologic runoffs, the study focuses on four scenarios related to the tidal range and runoffs: releases have been done at the beginning of spring tides and neap tides, in winter and summer seasons during flood and weak runoff events. All of these simulations have been performed with realistic atmospheric forcings, even though wind direction and intensity are highly variable at mid-latitude. First, it is challenging to find 15-day wind sequences that characterize the local atmospheric forcings. Second, the bay has a macro-tidal regime, so the water is mixed, whatever the weather conditions. We then focus on the two dominant runoff regimes (flood water vs low runoff) combined with the initial phase of the tide (spring vs neap tides) as detailed in Table 4.

a déplacé (et inséré) [4]

a supprimé: There are numerous indicators of hydrological characteristics based on theories of transport timescales. Over the years, many studies (Bolin and Rodhe, 1973; Zimmerman, 1976; Monsen et al., 2002; Takeoka, 1984) have defined and assessed different scales to describe water renewal on a particular spatial scale (a bay, an estuary, a harbour) in which mixing processes will renew the water mass (through open-ocean-connected boundaries or forced by runoff inputs). However, the vocabulary remains very diverse (Bacher et al., 2016). Those time scales are often provided in the framework of the constituent-oriented age and residence time theory (CART, www.climate.be/cart), under different names depending on their exact purpose (Deleersnijder et al., 2001; Delhez, 2006; Delhez et al., 2004; de Brauwere et al., 2011). They can also be used to specify the transport in the vertical direction (Meier, 2005; White, 2007; Bendtsen et al., 2009). (Lucas and Deleersnijder, 2020) have made a specific review of the whole set of indicators estimated either with Eulerian method or Lagrangian computation with particle-tracking. Most of these timescales can be averaged over the whole basin or can be defined locally, at every position in the basin, to provide a more detailed spatially distributed information on the water renewal capacity of a basin (Jouan et al., 2006). Moreover, under certain physical circumstances (large diffusion processes and weak runoffs), they can be identical (Viero and Defina, 2016b). * (... [70])

a supprimé: . It estimates

a supprimé: time scale

a supprimé: a

a supprimé: tracer released within a control domain. It ind (... [71])

a déplacé vers le haut [4]: 8).

a supprimé: volume of the bay plus the external part linke (... [72])

a supprimé: The return flow through the Goulet due to the (... [73])

a supprimé: elsewhere. After the release, only waters

a supprimé: are fixed with

a supprimé: then

a supprimé: The back-and-forth flow through the control (... [74])

a supprimé: (Plus et al., 2009),

a supprimé: tracers are separately released

a supprimé: .

a supprimé: an

a supprimé: solutions

a supprimé: 2

a supprimé: with respect

a supprimé: combined with two different

a supprimé: Releases

a supprimé: a

a supprimé: a low-flow

a supprimé: . A

a supprimé: description of the scenarios is given

Table 4: Environmental condition for each computation periods mean over the first 30 days of simulation

Scenario	Initial dates of <u>modeling</u>	Cumulated Aulne river flow (10 ⁶ m ³)	Wind velocity ± SD (m.s ⁻¹) and direction (°)
Low <u>runoff</u> – Neap tide	Jan 29 th 2016	380.3	8.43 ± 4.0 (257°)
Low <u>runoff</u> – Spring tide	Feb 6 th 2016	337.7	8.29 ± 4.2 (274°)
Flood – Neap tide	Aug 8 th 2015	13.7	4.69 ± 2.6 (281°)
Flood – Spring tide	Jul 29 th 2015	10.5	4.97 ± 2.7 (242°)

4.4. Flushing times of the Bay of Brest

490 The question addressed here is to evaluate the capability of MARS3D/AGRIF tool for characterizing the renewal capacity of the bay and identify the role played by the tidal forcing and river runoffs. The indicators have been estimated with both nesting methods for the four scenarios. The flushing times of the whole control volume are given in Table 5. As expected, low river runoffs imply a longer renewal time than flood situations. However, the initial tidal phase is the main change factor between the scenarios, with more intensive mixing during spring tides. There is a positive offset (roughly 10%) of the renewal time 495 from AGRIF two-way simulations. This shift is due to the return flow within the bay during each tidal cycle which is underestimated in the one-way model as its boundaries act as a sink for the tracer.

Table 5: Global e-folding flushing times and standard deviation in days for the whole control volume for both modeled configurations. The deviation is estimated over the 13 time released simulations for each scenario.

Scenario	Global <u>e-folding</u> flushing time in days	
	one-way	two-way
Low <u>runoff</u> – Neap tide	11.29 ± 0.42	12.23 ± 0.64
Low <u>runoff</u> – Spring tide	7.68 ± 0.39	8.34 ± 0.48
Flood – Neap tide	10.22 ± 0.41	10.84 ± 0.53
Flood – Spring tide	6.95 ± 0.35	7.85 ± 0.53

500 The local e-folding flushing times estimated with the two-way nesting configurations are displayed in Fig. 9 for the four scenarios. The indicator increases as the geographic position moves away from the control volume boundary. In contrast to the global indicator, the runoff impact on the renewal capacity of the bay is obvious. In low river runoff conditions, the southeastern part of the bay is isolated from the rest. The local e-folding flushing time reaches more than 25 days in shallow

- a supprimé: modelling
- a supprimé: water
- a supprimé: water
- a supprimé: 3
- a supprimé: water
- a supprimé: on the renewal capacity of the bay. Although wind direction and intensity are highly variables at mid-latitude, it has been decided not to focus on meteorological effects because it is difficult to find 15-days wind sequences that characterize the local atmospheric forcings. In addition, the bay is a highly energetic coastal area with strong diffusive and dispersive characteristics as its regime is macro-tidal. Then, the focus is on the two dominan (... [75])
- a supprimé: renewal indicator has
- a supprimé: For each simulation, this timescale features th (... [76])
- a supprimé: water
- a supprimé: larger
- a supprimé: compared to
- a supprimé: situation
- a supprimé: of change
- a supprimé: a
- a supprimé: in
- a supprimé: when
- a supprimé: nesting is used for the estimation of this indicator.
- a supprimé: inside
- a supprimé: that
- a supprimé: water
- a supprimé: water
- a supprimé: configuration in low-water conditions
- a supprimé: for initial spring tide (
- a supprimé: a) and neap tide (Fig. 9b). In
- a supprimé: same way, the renewal
- a supprimé: is shown for flood conditions for initial sprin (... [77])
- a supprimé: with
- a supprimé: relative to the border of
- a supprimé: opposition
- a supprimé: computation of
- a supprimé: here
- a supprimé: of runoff is clearly visible in
- a supprimé: water condition
- a supprimé: south-eastern
- a supprimé: clearly
- a supprimé: range of

1560 coves for a release at neap tide. The impact of tide is the next level in order of importance with, not surprisingly, stronger renewal during spring tide than neap tide. In each scenario, the central energetic eddy stands out because it is the rallying point of continental waters.

565 The relative differences in local e-folding flushing time estimates are illustrated in Fig. 10. Whatever the environmental conditions, the one-way nesting overestimates the renewal capacity of the bay by predicting lower local e-folding flushing times nearly everywhere. Such bias is expected because the one-way nesting does not correctly follow the tidal prism in the control volume: any tracers that leave the volume is lost for the estimate of the e-folding flushing time. In the inner part of the bay, the local differences are always negative and reach around 20% in flood conditions. Under low river runoff conditions, the renewal time is independent of the tide regime in the central part. In this area, the water mass is always replaced by the inflow during the period of simulation, so the treatment at the open boundary does not matter. In contrast, e-folding flushing time estimates are underestimated in shallow areas, especially during spring tides. To ensure that the disparities are due to open boundary treatment, a similar experiment was run with a much smaller control volume located only within the bay. Then 570 the simulated domain is larger than the control volume, and the results are identical regardless of the nesting method. This highlights the asset of the two-nesting for the evaluation of the water renewal times. Lastly, some suspicious patches appear at the western part of the control volume, which only takes into account tidal inputs. Others are visible next to the river mouths. Both are related to the initial time release and inaccurate exponential regression as the inflow quickly replace the initial water masses, as confirmed by (de Brauwere et al., 2011). 575

5. Discussion

580 The first objective of grid refinement is either to tackle a local stationary problem or to follow a single dynamical structure along with its displacements (Blayo and Debreu, 1999). In the MARS3D structured grid model, zooms allow reaching a resolution commensurable with the Rossby internal radius or with the coastal geometry in the presence of islands, capes or peninsulas. Unfortunately, the use of the ADI algorithm in MARS3D makes the implementation of the two-way AGRIF nesting tricky. In addition, coastal applications require the management of wet-drying. Still, the present applications demonstrate the capabilities of MARS3D/AGRIF two-way nesting to represent the macro-tidal dynamics and propagate the tracers in coastal areas. They also illustrate how it improves the monitoring of the fate of coastal water.

585 Despite the regular improvement in the computational power available for high-performance scientific computing, the computational cost and the storage of massive datasets remain significant issues for long-term numerical oceanic simulations due to various reasons, such as green computing considerations. We hereafter review the different key advantages provided by the introduction of the AGRIF library in MARS3D.

Regarding parametrization, the AGRIF library allows specifying different forcings (meteorology, runoff) or numerical schemes for each grid of the hierarchy. Consequently, the parameterizations can fit every local process. In addition, the local

a supprimé: Some particular structures appear at the western part of the control volume. This is due to a weak exponential regression where the residuals between exponential decay and simulation result are below 0.5. This part of the domain was only there to account for the tidal prism extent. A similar issue occurs next to the river mouths. Both problems are due to the initial time release over the first tide cycle. This is easily understandable for areas next to the volume limits in the ocean. For river mouth, (de Brauwere et al., 2011) pointed out that initial time release in estuaries could lead to extreme different values, as it is here between a release at high tide and low tide. However, the fact of considering the initial flushing lag (ranging from few hours up to 7 days) in each mesh strengthened considerably the e-folding regression approach. With one-way nesting, the ...he relative differences of ... [78]

a supprimé: for each mesh...imates are shown...llustrated in Fig. 10 in the same order than Fig. 9. First, spring (Fig. 10a) and neap (Fig. 10b) tides in low water condition and second spring (Fig. 10c) and neap (Fig. 10d) tides in flood condition. The one-way nesting overestimates in each cases ... Whatever the environmental the one-way nesting overestimates the renewal capacity of the bay by predicting lower local ... [79]

a mis en forme : Accentuation, Police :Non Italique, Couleur de police : Couleur personnalisée(RVB(14;16;26))

a mis en forme : Accentuation, Police :Non Italique, Couleur de police : Couleur personnalisée(RVB(14;16;26))

a supprimé: time...imes nearly everywhere. Such bias is expected because the one-way nesting does not correctly follow the tidal prism in the control volume: any tracers that leave the volume is lost for the estimate of the e-folding flushing time. In the inner part of the bay, the local differences are always negative and reach around 20% in flood conditions. Under low water condition, although there are no changes for...river runoff conditions, the energetic water mass...enewal time is independent of the tide regime in the central part, the discrepancies appear in the eastern part of the bay and... In this area, the water mass is always replaced by the inflow during the period of simulation, so the treatment at the open boundary does not matter. In contrast, e-folding flushing time estimates are ... [80]

a mis en forme : Couleur de police : Noir

a supprimé: The present study demonstrates the capabilities of MARS3D/AGRIF two-way nesting. The very...he first objective of grid refinement is either to tackle a local stationary problem or to follow a single dynamical structure along to ... [81]

a supprimé: The zoom is there to reach...n the MARS3D structured grid model, zooms allow reaching a relevant ...esolution (e.g., ...ommensurable with the Rossby internal radius or with the coastal geometry in the presence of a given structure or set of structures such as ...slands, capes or peninsulas) raising the ... [83]

a mis en forme ... [82]

a supprimé: huge...assive datasets remain major...ignificant issues for long-term numerical oceanic simulations,...due to various reasons, such as green computing considerations. We hereafter review the different key advantages provided by the introduc... [84]

a supprimé: the specification of a distinctive parametrisation...pecifying different forcings (meteorology, runoff) or numerical schemes for each grid of the hierarchy (meteorological forcings, runoff, vertical turbulence scheme, surface and bottom friction coefficients...). Consequently, the parameterization... [85]

time refinement is specific to each grid (ratio of 3 to 5). The more the dynamics are intense, the more the time refinement factor is increased.

The AGRIF flexibility also lies in the way child grids of a given hierarchy can be either added or easily removed. An offline bathymetric update tool, available with MARS3D code, modifies both mother and child bathymetries to fit fluxes (from one grid to another) along child borders. Once the bathymetry consistency is performed, users can launch the runs without additional tasks. The initial conditions for the new zoom are estimated online by the AGRIF library. This capability has been used to study more precisely the deep convection in the northwestern Mediterranean Sea (Garreau and Garnier, 2015) or to better identify the shear stress on marine renewable energy structures (Maisonnieu, Pers. comm). If user needs to remove a specific child grid, he simply has to recompute the bathymetry of the mother grid with the tool before launching the model.

The usual offline nesting procedure requires writing and storing of 3D forcing files from which the open boundary and initial conditions for the child grid are supplied. To prevent aliasing or spurious incompatibilities between barotropic and baroclinic modes, high frequency outputs must be saved to hard drive. Everywhere tidal dynamics are dominant, it involves a massive amount of I/O, which raises other kinds of issues, such as how to write massive data in a massive parallel context. Despite the many improvements to deal with this question, like deporting the I/O on dedicated CPUs with XIOS library (Yepes-Arbó et al., 2022), the cost of long-term storage of massive data, cannot be escaped. The on-the-fly grid nesting procedure (encompassing initial and open boundaries management) included in the two-way nesting circumvents these tedious steps by performing them online at each time step, and for the different grids of the hierarchy.

Another point concerns the vertical coordinate framework which is here a sigma one in MARS3D. The vertical interpolation towards a sigma framework often requires the projection onto a geopotential framework to perform a split horizontal-vertical interpolation. Such split interpolations on temperature and salinity fields can lead to gravity instabilities in case of significant bathymetric inconsistencies between the coarse and child grids. Therefore, the user must carefully define the interpolation parameters (such as those defining the intermediate geopotential framework onto which the vertical interpolation is performed) and check the consistency of the gravity gradient. As MARS3D/AGRIF two-way nesting requires a perfect fitting of the vertical discretization of all grids of the hierarchy and bathymetries coherence, these constraints prevent the gravity issues. Of course, this well-known problem may also be avoided in offline embedment procedures by taking the same care in defining the grid and the bathymetry computations.

The traditional one-way nesting remains a lighter solution than AGRIF two-way, especially in case repeated experiments are required for tuning purposes with different parametrizations or for exploring several environmental hypotheses (Cadier et al., 2017; Petton et al., 2020; Gangnery et al., 2019). As open boundary files can be re-used at no cost, this method still is a good approach to improve numerical developments in coastal models. However, the two-way update process is compulsory when the final objective is to ensure a conservative approach (biological tracer, connectivity study...) over large geographic areas at minimum cost. It is not a unique solution, as other kinds of spatial discretization such as unstructured, curvilinear or polar-style coordinates meet the same numerical constraints. The two-way nesting proposed here keeps it simple for the end user.

a supprimé: performed to fit to the local dynamics: ...pecific to each grid of the hierarchy can have its own sub-temporal integration as used in the regional configuration ...ratio of 3 to 5). The more the dynamics is...re intense, the more the time refinement factor is increased. Whereas for areas where the stability condition is more binding, the time refinement factor can be diminished. (... [86])

a mis en forme : Couleur de police : Automatique

a supprimé: grid in...rids of a given hierarchy can be either added or easily removed: the addition of a grid requires the coupling of this additional child grid bathymetry with the bathymetries of the other grids.... An offline bathymetric update algorithm...ool, available MARS3D code, modifies both mother and child bathymetries in order...to fit fluxes (from one grid to another) along child borders. Once the bathymetry consistency is performed along the boundaries between the mother and child grids, the user... users can launch the runs without additional tasks. The initial conditions for the new zoom are estimated online at the first timestep ...y the AGRIF library. This capability has been used to study more precisely the deep convection in the northwestern mediterranean sea (... [87])

a mis en forme (... [88])

a supprimé: over future...n marine renewable marine ...nergy structures (Maisonnieu, Pers. comm). In situations where the...f user needs to remove a specific child grid, he simply has to recompute the bathymetry of the mother grid's bathymetry has just to be recomputed (... [89])

a supprimé: storage...toring of 3D forcing files from which the open boundary and initial conditions for the child grid are supplied. In order to avoid...o prevent aliasing or spurious incompatibilities between barotropic and baroclinic modes, high ...frequency output...utputs must be saved to hard disk is required; in the most penalizing cases, for example where...rive. Everywhere tidal dynamics are dominant, it involves a huge... assive amount of I/O, which raises other kinds of issues, such as how to write massive data in a massive parallel context. Despite the many improvements to deal with this question, like deporting the I/O on dedicated CPUs as it is the case in the (... [90])

a mis en forme : Anglais (E.U.)

a supprimé: they cannot escape ...he cost of long-term storage of massive data. This is even more obvious in case of several nested grids in the same mother grid (such as the Bay of Biscay configuration) which would extend the pre-processing step to (... [91])

a mis en forme : Anglais (E.U.)

a supprimé: framework...one in MARS3D. The vertical interpolation towards a sigma framework often requires most of the time ...he projection onto a geopotential framework in order (... [92])

a mis en forme : Couleur de police : Texte 1

a supprimé: one has to perform ...epeated experiments are required for tuning purpose...urposes with different parametrizations or different ...or exploring several environmental hypothesis (... [93])

a mis en forme : Anglais (E.U.)

a mis en forme : Anglais (E.U.)

a supprimé: important ...umerical developments in coastal model...odels. However, the two-way update process is needed...ompulsory when the final objective is to assure...n (... [94])

As shown in Sect. 3.2, the online interpolation from mother to child grid and the update process preserve the propagation of tidal elevations and currents with an equivalent level of accuracy than the one achieved with the SHOM CST-France tidal forcing prescribed at open boundary conditions of a single typical coastal grid (some tens of kilometers of extension, in 10 to 100 m depth, at some hundreds of meters of resolution). The observed differences between the two-way nesting and the one-way offline methods are less than a few centimeters which are not significant in coastal areas. It is thus a real performance. First, because in the two-way nesting approach depicted here, the tidal propagation computed at the coarse grid level is fed with FES global reference tidal solution (Lyard et al., 2021) far away from the coasts. Second, because the use of the ADI algorithm requires that the coarse solution be updated over the entire child domains from the spatial average of their fine solutions. Therefore, it proves that the MARS3D/AGRIF implementation conserves mass and momentum and that the interactions between the child grids are handled accurately at open-sea and over wet-drying areas. In conclusion, MARS3D/AGRIF represents tides at regional and coastal scales, and at medium resolution (Lazure et al., 2009; Muller et al., 2014). It is well suited for large configurations with several zoom models, for long-term hindcast or operational forecast simulations to monitor the marine environment.

Regarding environmental applications, Sect. 4.3 confirms that the two-way nesting solution is mandatory to accurately estimate indicators characterizing the mixing within a bay, especially in macro-tidal regimes. For estimates defined over a control volume, the management of the open boundaries is a key element. On stand-alone grid, when the flow enters the domain, users can either choose to apply or nudge towards a constant value (zero or whatever value), a time series inferred from a large-scale solution (if available), or a zero-gradient condition. In all cases, the solution is strongly non-conservative, resulting in discrepancies in the final indicators. Even the one-way nesting is not conservative when the control volume is too close to an open boundary. Beyond the estimation of coastal indicators, the MARS3D/AGRIF two-way capability improves the management of the fate of a tracer outside the bay at the coarser horizontal resolution (and at fairly reasonable computational cost). It also enforces accurate incoming concentration across the open boundaries of the child grids. Such a conservative approach is relevant for applications with sediment, biological or chemical dynamics models.

Finally, it is worth noticing that such a software can also perform the opposite, that is, grid coarsening. It is a relevant capability for online physical-biogeochemical coupling. Such an approach has been used by (Lévy et al., 2012) in an offline mode. Capturing relevant scales of the oceanic flows may require higher spatial resolution than that required by the main biogeochemical features. For instance, the sub-mesoscale features enhance the vertical exchange and refuel the surface with nutrients. A few hundred meters spatial resolution is mandatory to simulate sub-mesoscale dynamics. But it is unaffordable for state-of-the-art biogeochemical models that use and advect tens of tracer fields (Heinze and Gehlen, 2013). The AGRIF coarsening capability allows this differential resolution (physics at high-resolution, biogeochemistry at lower resolution) by building online non-divergent transport fields from the high-resolution grid onto the coarse resolution grid. In that way, the "grand-mother" grid may completely overlap the mother grid.

- a supprimé: kilometres
- a supprimé: For this type of standalone grid, validated harmonic atlas at high horizontal resolution (Pineau-Guillou, 2013) may be available: enabling to represent accurately
- a supprimé: tidal elevations
- a supprimé: currents within
- a supprimé: encompassed area. According to the slow varying characteristics of the tidal components this downscaling approach can be thought to be performed only once by generating
- a supprimé: reference tidal atlas. In
- a supprimé: a
- a supprimé: either TPXO (Egbert and Erofeeva, 2002) or FES
- a supprimé: . For the regional configuration exposed previously, the tide coming
- a supprimé: mother grid with the two-way nesting has been only computed with the global FES model. The observed differences between the one-way offline and the two-way nesting methods are less than a few centimetres which are not really significant in coastal areas. It relies mainly on the continuity
- a supprimé: mass fluxes at the interface between the child and
- a mis en forme : Anglais (E.U.)
- a mis en forme : Anglais (E.U.)
- a supprimé: grids. This functionality is preserved thanks to the AGRIF library
- a supprimé: and allows MARS3D to represent
- a mis en forme : Anglais (E.U.)
- a déplacé vers le bas [5]: In that way, the "grand-mother" grid may completely overlap the mother grid.¶
- a supprimé: ¶ This software also has the capability to perform the opposite, that is to say grid coarsening. It is a relevant capability for on-line physical-biogeochemical coupling which was used for example by (Lévy et al., 2012) in an offline mode. Capturing relevant scales of the oceanic flows may require higher spatial resolution than the main feature of biogeochemical fields. In such a case, it is essential to solve the submesoscale features that enhance the vertical exchange and consequently refuel the surface with nutrients. The required resolution, of the order of a few hundred meters, is unaffordable for state-of-the-art biogeochemical models that use and advect tens of tracers fields (Heinze and Gehlen, 2013). The AGRIF coarse (... [95])
- a supprimé: In contrast, another perspective for the AGRIF (... [97])
- a mis en forme : Anglais (E.U.)
- a mis en forme (... [96])
- a mis en forme : Couleur de police : Automatique
- a mis en forme : Couleur de police : Automatique
- a supprimé: The AGRIF implementation in the MARS3D (... [98])
- a déplacé (et inséré) [5]
- a mis en forme (... [99])

Appendices

A. Data used for validation

The tidal validation is based on four stations from the French tidal gauge network RONIM maintained by the SHOM.

2410 Moreover, three datasets are available in the framework of the national program COAST-HF (Coastal Ocean Observing System-High Frequency, www.coast-hf.fr) which gathers fourteen automated moored buoys. The COAST-HF ASTAN buoy (48.749°N; 3.961°W) is a cardinal buoy of opportunity located 3.1 km offshore from Roscoff, east of the Batz Island. It records data every 30 minutes at 5-meter depth since 2008 (Gac et al., 2020), over a mean bathymetry of 45 m. The COAST-HF MAREL-Iroise buoy (48.357°N, 4.582°W) is located at the entrance of the bay of Brest and records data every 20 minutes at 2415 2-meter depth since 2000 (Rimmelin-Maury et al., 2020). Inside the bay of Brest next to the Mignonne river mouth, the COAST-HF SMART-Daoulas buoy (48.317°N, 4.331°W) is monitoring parameters at 50 cm over the seabed at 15-mins frequency since 2016 (Petton et al., 2021b). Next to this last point, the Ifremer observatory network ECOSCOPA has a study site called Pointe du Château (48.335°N, 4.319°W) on an oyster farm in the intertidal zone. Temperature and salinity data are available at a 15-mins frequency since 2008 (Petton et al., 2021a). We also had access to the sea surface temperature data from 2420 the Datawell buoy of les Pierres Noires which is part of the swell monitoring network CANDHIS (CEREMA) and located in the middle of the Iroise Sea (48.29°N, 4.97°W). These monitoring stations are presented in Fig. 5 and Fig. 8.

Besides, satellite data are used for sea surface temperature validation at two different horizontal scales: The first one is based on SST fields extracted from the global Advanced Very High Resolution Radiometer (AVHRR) Pathfinder V5 daily dataset.

2425 The ODYSSEA chain has been modified by (Saulquin and Gohin, 2010) to use optimal interpolation for the reconstruction of gap-free and using the previous analysis as a first guess. The product is gridded at a 0.02° spatial resolution and freely available at <https://resources.marine.copernicus.eu> (Autret and Piollé, 2018). The second one is based on the Thermal InfraRed Sensor (TIRS) from the Landsat 8 satellite. As it orbits the Earth in a sun-synchronous, near-polar orbit inclined at 98.2 degrees, one gets a track over our area of interest every 8 days. Consequently, it is hard to extract snapshots without too much clouds. Recently the United States Geological Survey (USGS) has started to distribute Landsat Collection 2 Level 2 (values are given 2430 after atmospheric corrections) with a calibrated land surface temperature field. The development of a water temperature algorithm is not the aim of this paper and represents a challenge by itself (Vanhellemont, 2020). However, the use of such high-resolution product (30m gridded) is very useful to detect fine structures. In that respect, the ODYSSEA product is complementary to the Landsat 8 scene and a reference on a coarser grid. To discriminate water temperature from cloud or land value, the quality index given for each pixel for this collection is used.

2435 Code availability

Last version of MARS3D is freely available on request at <https://wwz.ifremer.fr/mars3d/>. The AGRIF library is freely available at under CECILL license (<http://www.cecill.info>). Both codes are written in Fortran-90/95 and figures are displayed from

a mis en forme : Anglais (E.U.)

python scripts or with QGIS software for both configuration presentations. All the model code, bathymetric grid files, namelist configuration files for both regional and coastal applications and python scripts used in this paper are available at
2440 <https://doi.org/10.5281/zenodo.6672562>.

Data availability

All data used in this paper are freely available from their DOI repository.

Author contribution

LD has developed the AGRIF Library. LD, VG and FD have integrated the AGRIF library in the MARS3D model. MC and
2445 SP have setup the model configurations, adapted the AGRIF integration to coastal environment and provided figures for the paper. All authors have contributed to the concepts and the writing of the paper.

Competing interest

The contact author has declared that neither he nor their co-authors have any competing interests.

Financial support

2450 V. Garnier, F. Dumas and L. Debreu were funded by the French National Research Agency (ANR) through (COMODO). MARS3D - AGRIF capability has been implemented and funded within the framework of PREVIMER project to monitor the regional and coastal environmental dynamics.

References

- 2455 [Auffret, G.-A.: Dynamique sédimentaire de la marge continentale celtique - Evolution Cénozoïque - Spécificité du Pleistocène supérieur et de l'Holocène, Université de Bordeaux I, 1983.](#)
- [Autret, E. and Piollé, J.-F.: European North West Shelf/Iberia Biscay Irish Seas - High Resolution ODYSSEA L4 Sea Surface Temperature Analysis, <https://doi.org/https://doi.org/10.48670/moi-00152>, 2018.](#)
- 2460 [Berger, M. J. and Olinger, J.: Adaptive mesh refinement for hyperbolic partial differential equations, J Comput Phys, 53, 484–512, \[https://doi.org/https://doi.org/10.1016/0021-9991\\(84\\)90073-1\]\(https://doi.org/https://doi.org/10.1016/0021-9991\(84\)90073-1\), 1984.](#)
- [Bezaud, M. and Pineau-Guillou, L.: Qualification des modèles hydrodynamiques 3D des côtes de la Manche et de l'Atlantique, 158 pp., 2015.](#)

a mis en forme : Anglais (E.U.)

a supprimé: Bacher, C., Filgueira, R., and Guyonnet, T.: Probabilistic approach of water residence time and connectivity using Markov chains with application to tidal embayments, *Journal of Marine Systems*, 153, 25–41, <https://doi.org/10.1016/j.jmarsys.2015.09.002>, 2016.
Bendtsen, J., Gustafsson, K. E., Söderkvist, J., and Hansen, J. L. S.: Ventilation of bottom water in the North Sea–Baltic Sea transition zone, *Journal of Marine Systems*, 75, 138–149, <https://doi.org/10.1016/J.JMARSYS.2008.08.006>, 2009.

- Biastoch, A., Böning, C. W., Schwarzkopf, F. U., and Lutjeharms, J. R. E.: Increase in Agulhas leakage due to poleward shift of Southern Hemisphere westerlies, *Nature*, 462, 495–498, <https://doi.org/10.1038/nature08519>, 2009.
- Biastoch, A., Sein, D., Durgadoo, J. V., Wang, Q., and Danilov, S.: Simulating the Agulhas system in global ocean models – nesting vs. multi-resolution unstructured meshes, *Ocean Model (Oxf)*, 121, 117–131, <https://doi.org/10.1016/j.ocemod.2017.12.002>, 2018.
- Blayo, E. and Debreu, L.: Adaptive Mesh Refinement for Finite-Difference Ocean Models: First Experiments, *J Phys Oceanogr*, 29, 1239–1250, [https://doi.org/10.1175/1520-0485\(1999\)029<1239:AMRFFD>2.0.CO;2](https://doi.org/10.1175/1520-0485(1999)029<1239:AMRFFD>2.0.CO;2), 1999.
- de Brauwere, A., de Brye, B., Blaise, S., and Deleersnijder, E.: Residence time, exposure time and connectivity in the Scheldt Estuary, *Journal of Marine Systems*, 84, 85–95, <https://doi.org/10.1016/j.jmarsys.2010.10.001>, 2011.
- Cadier, M., Gorgues, T., Sourisseau, M., Edwards, C. A., Aumont, O., Marié, L., and Memery, L.: Assessing spatial and temporal variability of phytoplankton communities' composition in the Iroise Sea ecosystem (Brittany, France): A 3D modeling approach. Part 1: Biophysical control over plankton functional types succession and distribution, *Journal of Marine Systems*, 165, 47–68, <https://doi.org/https://doi.org/10.1016/j.jmarsys.2016.09.009>, 2017.
- Inter annual hydrodynamic hindcast with MARS3D-AGRIF model - Bay of biscay and Manche Areas:
- Capet, X.: Contributions to the understanding of meso/submesoscale turbulence and their impact on the ocean functioning, UPMC - Université Paris 6 Pierre et Marie Curie, 2015.
- Debreu, L. and Blayo, E.: Two-way embedding algorithms: a review, *Ocean Dyn*, 58, 415–428, <https://doi.org/10.1007/s10236-008-0150-9>, 2008.
- Debreu, L., Vouland, C., and Blayo, E.: AGRIF: Adaptive grid refinement in Fortran, *Comput Geosci*, 34, 8–13, <https://doi.org/10.1016/j.cageo.2007.01.009>, 2008.
- Debreu, L., Marchesiello, P., Penven, P., and Cambon, G.: Two-way nesting in split-explicit ocean models: Algorithms, implementation and validation, *Ocean Model (Oxf)*, 49–50, 1–21, <https://doi.org/https://doi.org/10.1016/j.ocemod.2012.03.003>, 2012.
- Delandmeter, P., Lambrechts, J., Legat, V., Vallaey, V., Naithani, J., Thiery, W., Remacle, J.-F., and Deleersnijder, E.: A fully consistent and conservative vertically adaptive coordinate system for SLIM 3D v0.4 with an application to the thermocline oscillations of Lake Tanganyika, *Geosci Model Dev*, 11, 1161–1179, <https://doi.org/10.5194/gmd-11-1161-2018>, 2018.
- Diaz, M., Grasso, F., Le Hir, P., Sottolichio, A., Caillaud, M., and Thouvenin, B.: Modeling Mud and Sand Transfers Between a Macrotidal Estuary and the Continental Shelf: Influence of the Sediment Transport Parameterization, *J Geophys Res Oceans*, 125, e2019JC015643, <https://doi.org/https://doi.org/10.1029/2019JC015643>, 2020.
- Dufois, F., Verney, R., Le Hir, P., Dumas, F., and Charmasson, S.: Impact of winter storms on sediment erosion in the Rhone River prodelta and fate of sediment in the Gulf of Lions (North Western Mediterranean Sea), *Cont Shelf Res*, 72, 57–72, <https://doi.org/https://doi.org/10.1016/j.csr.2013.11.004>, 2014.

a supprimé: Bolin, B. and Rodhe, H.: A note on the concepts of age distribution and transit time in natural reservoirs, *Tellus*, 25, 58–62, <https://doi.org/10.1111/j.2153-3490.1973.tb01594.x>, 1973.

a supprimé: Debreu, L., Auclair, F., Benshila, R., Capet, X., Dumas, F., Julien, S., and Marchesiello, P.: Multiresolution in CROCO (Coastal and Regional Ocean Community model), in: EGU General Assembly Conference Abstracts, EPSC2016-15272, 2016.

a supprimé: Deleersnijder, E., Campin, J.-M. M., and Delhez, E. J. M.: The concept of age in marine modelling I. Theory and preliminary model results, *Journal of Marine Systems*, 28, 229–267, [https://doi.org/10.1016/S0924-7963\(01\)00026-4](https://doi.org/10.1016/S0924-7963(01)00026-4), 2001.

Delhez, E. J. M.: Transient residence and exposure times, *Ocean Science*, 2, 1–9, <https://doi.org/10.5194/os-2-1-2006>, 2006.

Delhez, E. J. M., Heemink, A. W., and Deleersnijder, E.: Residence time in a semi-enclosed domain from the solution of an adjoint problem, *Estuar Coast Shelf Sci*, 61, 691–702, <https://doi.org/10.1016/j.ecss.2004.07.013>, 2004.

- Egbert, G. D. and Erofeeva, S. Y.: Efficient Inverse Modeling of Barotropic Ocean Tides, *J Atmos Ocean Technol*, 19, 183–204, [https://doi.org/10.1175/1520-0426\(2002\)019<0183:EIMOBO>2.0.CO;2](https://doi.org/10.1175/1520-0426(2002)019<0183:EIMOBO>2.0.CO;2), 2002.
- Fiandrino, A., Ouisse, V., Dumas, F., Lagarde, F., Pete, R., Malet, N., Le Noc, S., and de Wit, R.: Spatial patterns in coastal lagoons related to the hydrodynamics of seawater intrusion, *Mar Pollut Bull*, 119, 132–144, <https://doi.org/10.1016/j.marpolbul.2017.03.006>, 2017.
- Frère, L., Paul-Pont, I., Rinnert, E., Petton, S., Jaffré, J., Bihannic, I., Soudant, P., Lambert, C., and Huvet, A.: Influence of environmental and anthropogenic factors on the composition, concentration and spatial distribution of microplastics: A case study of the Bay of Brest (Brittany, France), *Environmental Pollution*, 225, 211–222, <https://doi.org/10.1016/j.envpol.2017.03.023>, 2017.
- Gac, J.-P., Marrec, P., Cariou, T., Guillerm, C., Macé, É., Vernet, M., and Bozec, Y.: Cardinal Buoys: An Opportunity for the Study of Air-Sea CO₂ Fluxes in Coastal Ecosystems, *Front Mar Sci*, 7, <https://doi.org/10.3389/fmars.2020.00712>, 2020.
- Gangnery, A., Normand, J., Duval, C., Cugier, P., Grangeré, K., Petton, B., Petton, S., Orvain, F., and Pernet, F.: Connectivities with Shellfish Farms and Channel Rivers are Associated with Mortality Risk in Oysters, *Aquac Environ Interact*, 11, 493–506, <https://doi.org/10.3354/aei00327>, 2019.
- Garreau, P. and Garnier, V.: Physical processes acting in a numerical oceanic model during the convection period of SOP2, in: 9th HyMeX workshop, 21–25 September 2015, Mykonos, Greece, Oral, 2015.
- Grasso, F., Verney, R., Le Hir, P., Thouvenin, B., Schulz, E., Kervella, Y., Khojasteh Pour Fard, I., Lemoine, J.-P., Dumas, F., and Garnier, V.: Suspended Sediment Dynamics in the Macrotidal Seine Estuary (France): 1. Numerical Modeling of Turbidity Maximum Dynamics, *J Geophys Res Oceans*, 123, 558–577, <https://doi.org/https://doi.org/10.1002/2017JC013185>, 2018.
- Grifoll, M., Del Campo, A., Espino, M., Mader, J., González, M., and Borja, Á.: Water renewal and risk assessment of water pollution in semi-enclosed domains: Application to Bilbao Harbour (Bay of Biscay), *Journal of Marine Systems*, 109–110, S241–S251, <https://doi.org/10.1016/j.jmarsys.2011.07.010>, 2013.
- Heinze, C. and Gehlen, M.: Modeling Ocean Biogeochemical Processes and the Resulting Tracer Distributions, in: *Ocean Circulation and Climate*, vol. 103, edited by: Siedler, G., Griffies, S. M., Gould, J., and Church, J. A. B. T.-I. G., Academic Press, 667–694, <https://doi.org/10.1016/B978-0-12-391851-2.00026-X>, 2013.
- Huret, M., Sourisseau, M., Petitgas, P., Struski, C., Léger, F., and Lazure, P.: A multi-decadal hindcast of a physical-biogeochemical model and derived oceanographic indices in the Bay of Biscay, *Journal of Marine Systems*, 109–110, <https://doi.org/10.1016/j.jmarsys.2012.02.009>, 2013.
- Janin, J. M., Lepeintre, F., Pechon, P., and de France. Direction des études et recherches. Service Applications de l'électricité et environnement, E.: Telemac-3d: a Finite Element Code to Solve 3D Free Surface Flow Problems., EDF-DER, 1993.
- Jiang, C., Liu, Y., Long, Y., and Wu, C.: Estimation of Residence Time and Transport Trajectory in Tieshangang Bay, China, *Water (Basel)*, 9, 321, <https://doi.org/10.3390/w9050321>, 2017.

- 555 Jordi, A., Ferrer, M. I., Vizoso, G., Orfila, A., Basterretxea, G., Casas, B., Álvarez, A., Roig, D., Garau, B., Martínez, M., Fernández, V., Fornés, A., Ruiz, M., Fornós, J. J., Balaguer, P., Duarte, C. M., Rodríguez, I., Alvarez, E., Onken, R., Orfila, P., and Tintoré, J.: Scientific management of Mediterranean coastal zone: A hybrid ocean forecasting system for oil spill and search and rescue operations, *Mar Pollut Bull*, 53, 361–368, <https://doi.org/10.1016/j.marpolbul.2005.10.008>, 2006.
- Jouon, A., Douillet, P., Ouillon, S., and Fraunié, P.: Calculations of hydrodynamic time parameters in a semi-opened coastal zone using a 3D hydrodynamic model, *Cont Shelf Res*, 26, 1395–1415, <https://doi.org/10.1016/j.csr.2005.11.014>, 2006.
- 2560 Kininmonth, S. J., De'ath, G., and Possingham, H. P.: Graph theoretic topology of the Great but small Barrier Reef world, *Theor Ecol*, 3, 75–88, <https://doi.org/10.1007/s12080-009-0055-3>, 2010.
- Lazure, P. and Dumas, F.: An external–internal mode coupling for a 3D hydrodynamical model for applications at regional scale (MARS), *Adv Water Resour*, 31, 233–250, <https://doi.org/10.1016/J.ADVWATRES.2007.06.010>, 2008.
- 565 Lazure, P., Garnier, V., Dumas, F., Herry, C., and Chifflet, M.: Development of a hydrodynamic model of the Bay of Biscay. Validation of hydrology, *Cont Shelf Res*, 29, 985–997, <https://doi.org/10.1016/j.csr.2008.12.017>, 2009.
- Leendertse, J. J. and Gritton, E. C.: A water quality simulation model for well mixed estuaries and coastal seas: Vol. II, *Computation Procedures*, 1971.
- Lévy, M., Resplandy, L., Klein, P., Capet, X., Iovino, D., and Ethé, C.: Grid degradation of submesoscale resolving ocean models: Benefits for offline passive tracer transport, *Ocean Model (Oxf)*, 48, 1–9, <https://doi.org/https://doi.org/10.1016/j.ocemod.2012.02.004>, 2012.
- 2570 Li, J. G.: Filling oceans on a spherical multiple-cell grid, *Ocean Model (Oxf)*, 157, 101729, <https://doi.org/10.1016/j.ocemod.2020.101729>, 2021.
- Lyard, F. H., Allain, D. J., Cancet, M., Carrère, L., and Picot, N.: FES2014 global ocean tide atlas: design and performance, *Ocean Science*, 17, 615–649, <https://doi.org/10.5194/os-17-615-2021>, 2021.
- 575 Marchesiello, P., Capet, X., Menkes, C., and Kennan, S. C.: Submesoscale dynamics in tropical instability waves, *Ocean Model (Oxf)*, 39, 31–46, <https://doi.org/10.1016/j.ocemod.2011.04.011>, 2011.
- Muller, H., Blanke, B., Dumas, F., Lekien, F., and Mariette, V.: Estimating the Lagrangian residual circulation in the Iroise Sea, *Journal of Marine Systems*, 78, S17–S36, <https://doi.org/https://doi.org/10.1016/j.jmarsys.2009.01.008>, 2009.
- 580 Muller, H., Pineau-Guillou, L., Idier, D., and Ardhuin, F.: Atmospheric storm surge modeling methodology along the French (Atlantic and English Channel) coast, *Ocean Dyn*, 64, 1671–1692, <https://doi.org/10.1007/s10236-014-0771-0>, 2014.
- Naranjo, C., Garcia-Lafuente, J., Sannino, G., and Sanchez-Garrido, J. C.: How much do tides affect the circulation of the Mediterranean Sea? From local processes in the Strait of Gibraltar to basin-scale effects, *Prog Oceanogr*, 127, 108–116, <https://doi.org/https://doi.org/10.1016/j.pocean.2014.06.005>, 2014.
- 585 Neal, V. T.: PREDICTED FLUSHING TIMES AND POLLUTION DISTRIBUTION IN THE COLUMBIA RIVER ESTUARY, *Coastal Engineering Proceedings*, 1, 81, <https://doi.org/10.9753/jcece.v10.81>, 1966.
- Le Pape, O. and Menesguen, A.: Hydrodynamic prevention of eutrophication in the Bay of Brest (France), a modelling approach, *Journal of Marine Systems*, 12, 171–186, [https://doi.org/10.1016/S0924-7963\(96\)00096-6](https://doi.org/10.1016/S0924-7963(96)00096-6), 1997.

a supprimé: Lucas, L. V. and Deleersnijder, E.: Timescale Methods for Simplifying, Understanding and Modeling Biophysical and Water Quality Processes in Coastal Aquatic Ecosystems: A Review, *Water (Basel)*, 12, 2717, <https://doi.org/10.3390/w12102717>, 2020.

a supprimé: Marsaleix, P., Auclair, F., and Estournel, C.: Considerations on Open Boundary Conditions for Regional and Coastal Ocean Models, *J Atmos Ocean Technol*, 23, 1604–1613, <https://doi.org/10.1175/JTECH1930.1>, 2006. Meier, H. E. M.: Modeling the age of Baltic Seawater masses: Quantification and steady state sensitivity experiments, *J Geophys Res Oceans*, 110, <https://doi.org/10.1029/2004JC002607>, 2005. Monsen, N. E., Cloern, J. E., Lucas, L. V., and Monismith, S. G.: A comment on the use of flushing time, residence time, and age as transport time scales, *Limnol Oceanogr*, 47, 1545–1553, <https://doi.org/10.4319/lo.2002.47.5.1545>, 2002.

1605 Penven, P., Debreu, L., Marchesiello, P., and McWilliams, J. C.: Evaluation and application of the ROMS 1-way embedding procedure to the central california upwelling system, *Ocean Model (Oxf)*, 12, 157–187, <https://doi.org/https://doi.org/10.1016/j.ocemod.2005.05.002>, 2006.

Petton, S. and Dumas, F.: MARS3D / AGRIF model configuration for the Bay of Brest, <https://doi.org/10.17882/86400>, 18 February 2022.

1610 Petton, S., Pouvreau, S., and Dumas, F.: Intensive use of Lagrangian trajectories to quantify coastal area dispersion, <https://doi.org/10.1007/s10236-019-01343-6>, 2020.

Petton, S., Le Roy, V., Bellec, G., Queau, I., Le Souchu, P., and Pouvreau, S.: Marine environmental station database of Daoulas bay, <https://doi.org/10.17882/42493>, 2021a.

Petton, S., Le Roy, V., and Pouvreau, S.: SMART Daoulas data from coriolis Data Centre in the Bay of Brest, 2615 <https://doi.org/10.17882/86020>, January 2021b.

Pineau-Guillou, L.: PREVIMER. Validation des atlas de composantes harmoniques de hauteurs et courants de marée, Ifremer, Ifremer, France, 2013.

Piton, V., Herrmann, M., Lyard, F., Marsaleix, P., Duhaut, T., Allain, D., and Ouillon, S.: Sensitivity study on the main tidal constituents of the Gulf of Tonkin by using the frequency-domain tidal solver in T-UGOM, *Geosci Model Dev*, 13, 1583–2620 1607, <https://doi.org/10.5194/gmd-13-1583-2020>, 2020.

Plus, M., Dumas, F., Stanisière, J. Y., and Maurer, D.: Hydrodynamic characterization of the Arcachon Bay, using model-derived descriptors, *Cont Shelf Res*, 29, 1008–1013, <https://doi.org/10.1016/j.csr.2008.12.016>, 2009.

Rétif, F., Bouchette, F., Marsaleix, P., Liou, J.-Y., Meulé, S., Michaud, H., Lin, L.-C., Hwang, K.-S., Bujan, N., Hwung, H.-H., and Team, S.: REALISTIC SIMULATION OF INSTANTANEOUS NEARSHORE WATER LEVELS DURING 2625 TYPHOONS, *Coastal Engineering Proceedings*, 1, waves.17, <https://doi.org/10.9753/icce.v34.waves.17>, 2014.

Rimmelín-Maury, P., Charria, G., Repecaud, M., Quemener, L., Beaumont, L., Guillot, A., Gautier, L., Prigent, S., Le Becque, T., Bihannic, I., Bonnat, A., Le Roux, J.-F., Grossteffan, E., Devesa, J., and Bozec, Y.: Iroise buoy data from Coriolis data center as core parameter support for Brest Bay and Iroise sea studies, <https://doi.org/https://doi.org/10.17882/74004>, 2020.

Roelvink, J. A. D. and van Banning, G.: Design and development of DELFT3D and application to coastal morphodynamics, 2630 *Oceanographic Literature Review*, 11, 925, 1995.

Rossi, V., Ser-Giacomi, E., López, C., and Hernández-García, E.: Hydrodynamic provinces and oceanic connectivity from a transport network help designing marine reserves, *Geophys Res Lett*, 41, 2883–2891, <https://doi.org/10.1002/2014GL059540>, 2014.

le Roy, R. and Simon, B.: Réalisation et validation d'un modèle de marée en Manche et dans le Golfe de Gascogne. Application 2635 à la réalisation d'un nouveau programme de réduction des sondages bathymétriques, *Rapport technique, EPSHOM*, 2003.

Saulquin, B. and Gohin, F.: Mean seasonal cycle and evolution of the sea surface temperature from satellite and in situ data in the English Channel for the period 1986–2006, *Int J Remote Sens*, 31, 4069–4093, <https://doi.org/10.1080/01431160903199155>, 2010.

2640 | Thomas, C. J., Lambrechts, J., Wolanski, E., Traag, V. A., Blondel, V. D., Deleersnijder, E., and Hanert, E.: Numerical
modelling and graph theory tools to study ecological connectivity in the Great Barrier Reef, *Ecol Modell*, 272, 160–174,
<https://doi.org/10.1016/J.ECOLMODEL.2013.10.002>, 2014.

Vanhellemont, Q.: Automated water surface temperature retrieval from Landsat 8/TIRS, *Remote Sens Environ*, 237, 111518,
<https://doi.org/10.1016/j.rse.2019.111518>, 2020.

2645 | Viero, D. Pietro and Defina, A.: Renewal time scales in tidal basins: Climbing the Tower of Babel, *Sustainable Hydraulics in
the Era of Global Change*, 338–345, 2016.

Yepes-Arbós, X., van den Oord, G., Acosta, M. C., and Carver, G. D.: Evaluation and optimisation of the I/O scalability for
the next generation of Earth system models: IFS CY43R3 and XIOS 2.0 integration as a case study, *Geosci Model Dev*, 15,
379–394, <https://doi.org/10.5194/gmd-15-379-2022>, 2022.

2650 |

a supprimé: Takeoka, H.: Fundamental concepts of exchange and transport time scales in a coastal sea, *Cont Shelf Res*, 3, 311–326, [https://doi.org/10.1016/0278-4343\(84\)90014-1](https://doi.org/10.1016/0278-4343(84)90014-1), 1984. ¶

a supprimé: 2016a

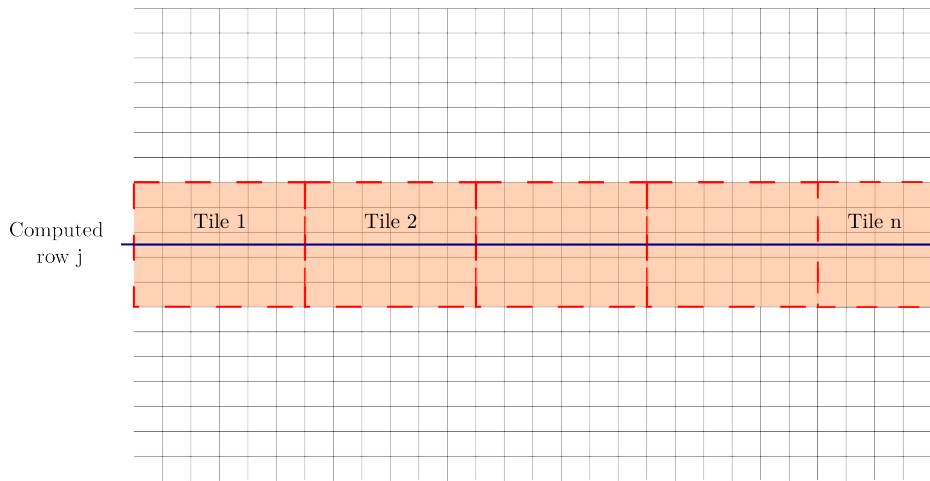
a supprimé: Viero, D. Pietro and Defina, A.: Water age, exposure time, and local flushing time in semi-enclosed, tidal basins with negligible freshwater inflow, *Journal of Marine Systems*, 156, 16–29, <https://doi.org/10.1016/j.jmarsys.2015.11.006>, 2016b. ¶
White, L.: Diagnoses of vertical transport in a three-dimensional finite element model of the tidal circulation around an island, *Estuar Coast Shelf Sci*, 74, 655–669, <https://doi.org/10.1016/J.ECSS.2006.07.014>, 2007. ¶

a supprimé: Zimmerman, J. T. F.: Mixing and flushing of tidal embayments in the western Dutch Wadden Sea part I: Distribution of salinity and calculation of mixing time scales, [https://doi.org/10.1016/0077-7579\(76\)90013-2](https://doi.org/10.1016/0077-7579(76)90013-2), 1 September 1976.

a supprimé: ¶

a mis en forme : Anglais (E.U.)

a mis en forme : Anglais (E.U.)



2670

Figure 1: Schematic domain decomposition for solving ADI equation system

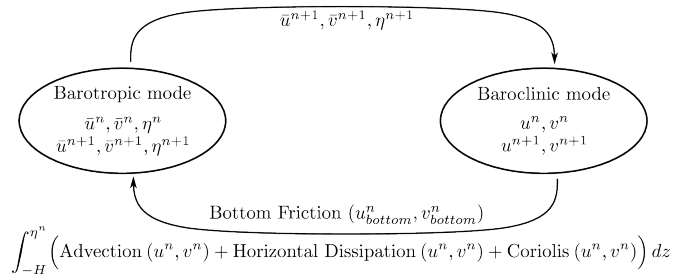


Figure 2: Diagram of the coupling between barotropic and baroclinic mode

2675

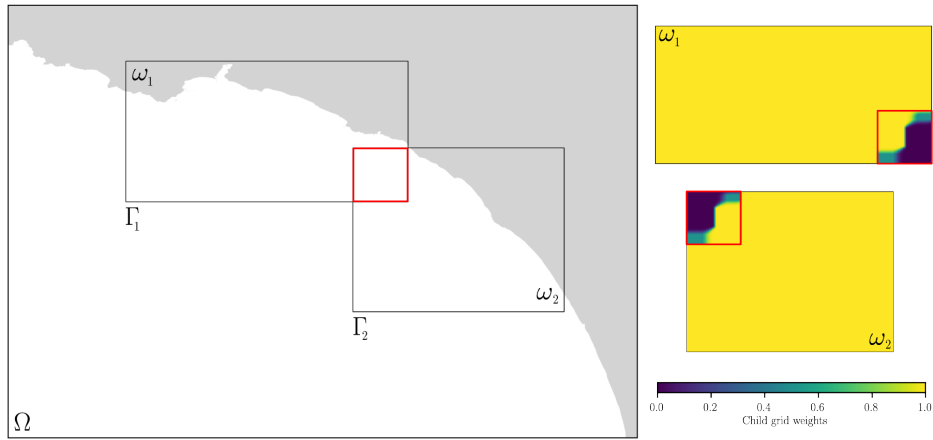
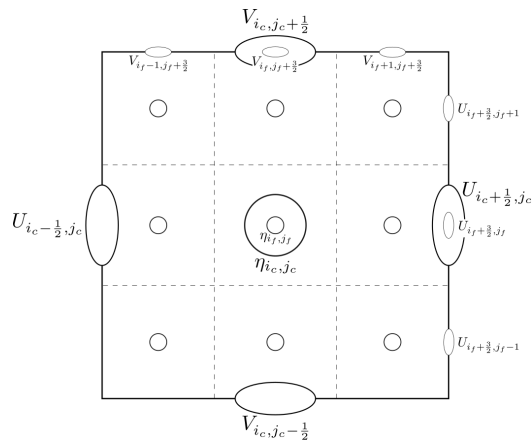


Figure 3: On the left, local refinement with two child grids. On the right, the weights used for interaction at same hierarchical level on the overlap area represented with a red rectangle.



2680 Figure 4: A coarse grid cell divided in nine fine grid cells on a C grid

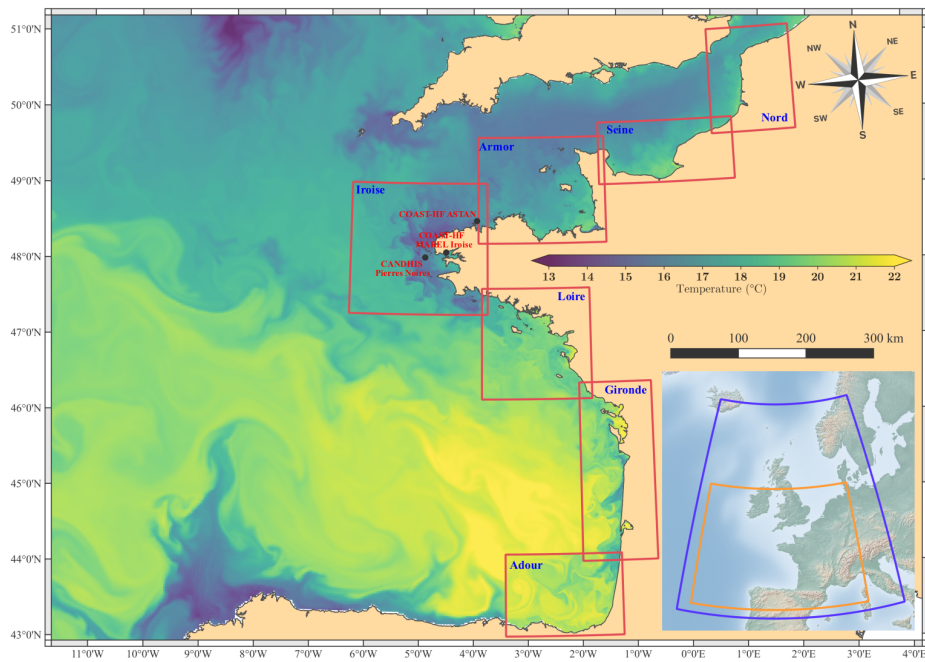
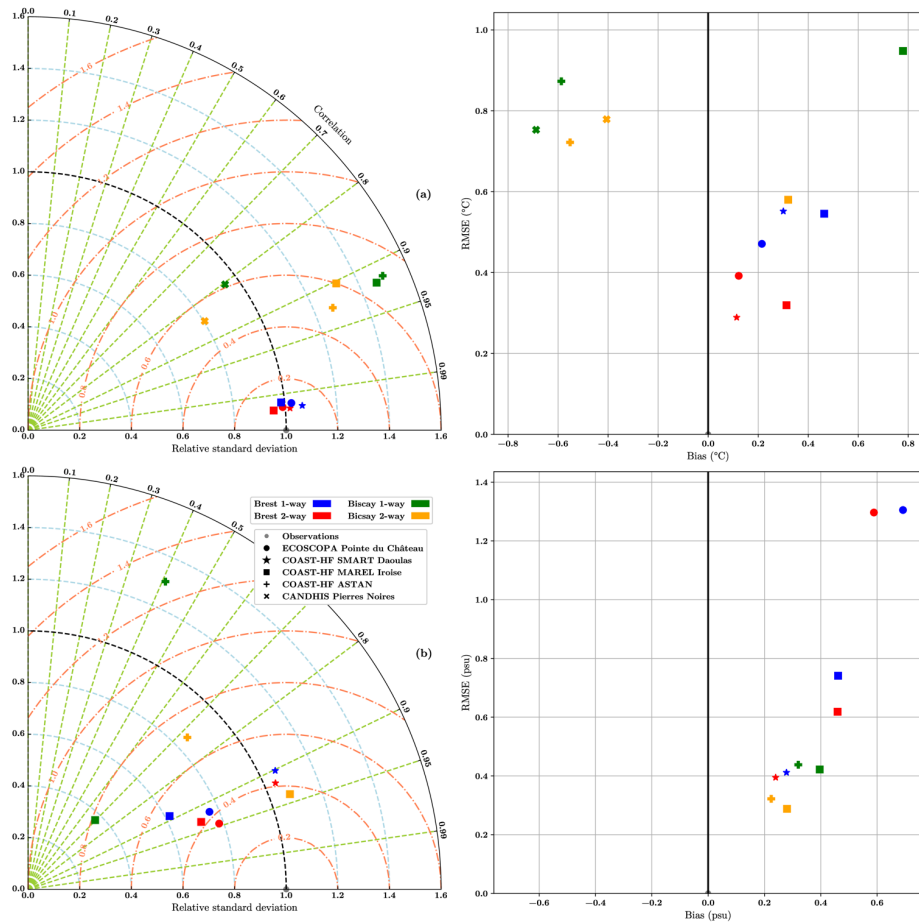
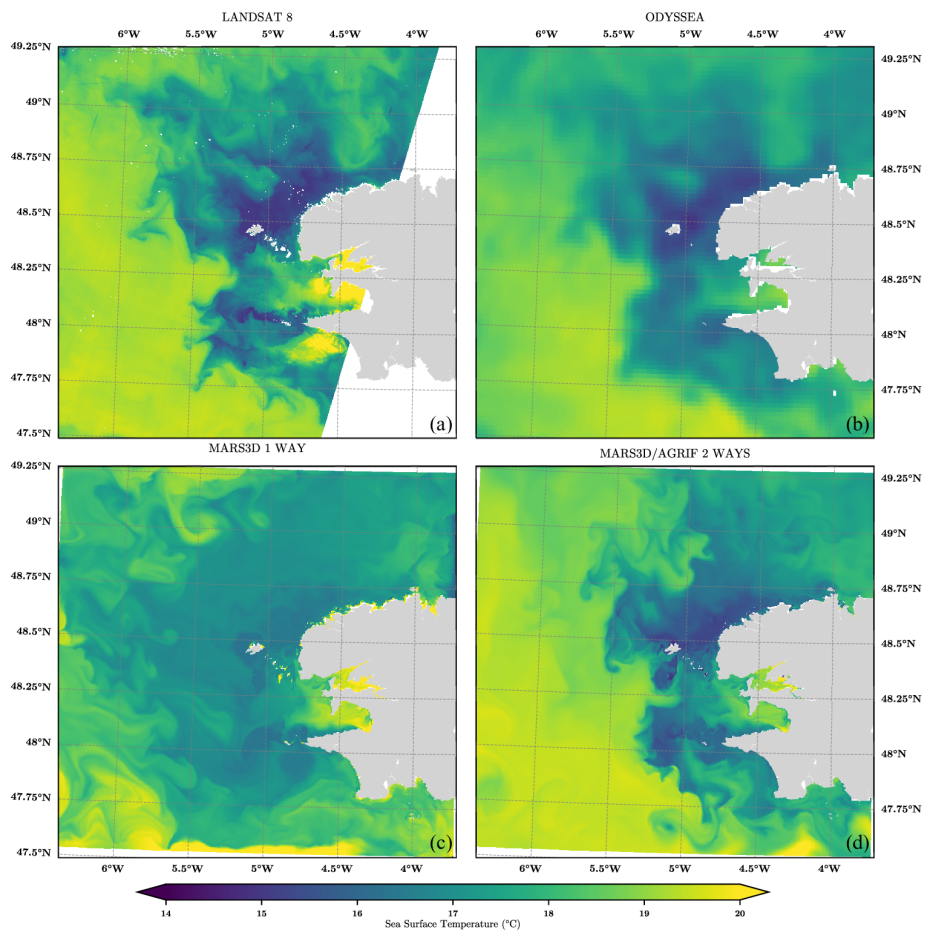


Figure 5: Bay of Biscay configuration with seven zooms of 500m resolution (red rectangles). The 2.5 km resolution coarser grid (orange rectangle) is included in a larger 2D model at 5 km resolution (blue rectangle). The sea surface temperature is given for the 16th august 2018 with the finest possible resolution. Bathymetric and coastline sources: Ifremer / SHOM / Natural Earth.



2685

Figure 6: Temperature (a) and Salinity (b) validation for both configurations. The Taylor diagrams are represented with relative standard deviation (blue dashed lines), correlation (green dashed lines) and relative root mean square error (red dashed lines).



2690 **Figure 7:** Sea surface temperature over the Iroise sea on August 15th, 2016 for Landsat 8 (a), Odyssea (b), one-way simulation (c) and two-way simulation (d). Coastline source: SHOM.

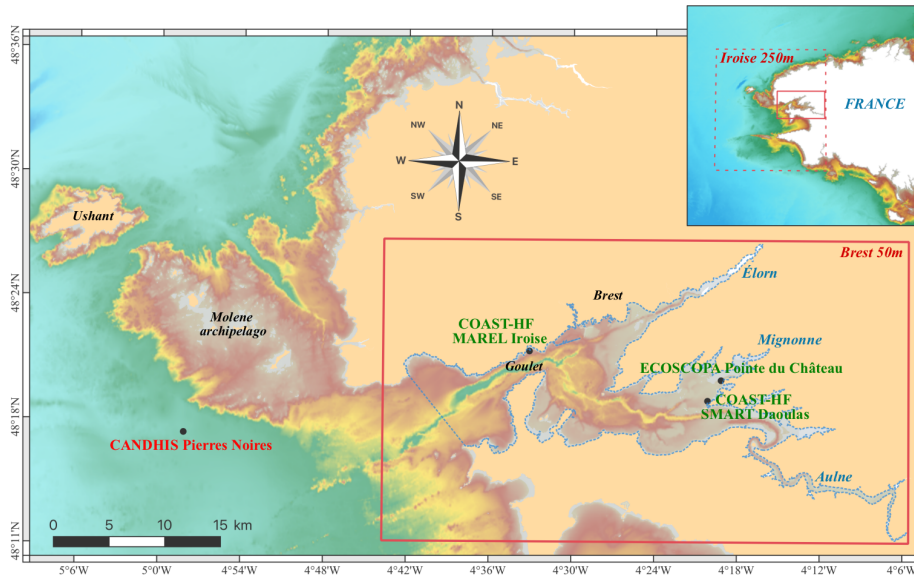


Figure 8: Bay of Brest configuration. The geographic extent of the zoom grid at 50 m resolution is the solid red rectangle. The coarser grid at 250 m resolution is the dashed red rectangle. The dashed blue line represents the control volume used for the estimation of the renewal indicator. Bathymetric and coastline sources: Ifremer / SHOM.

695

a mis en forme : Taquets de tabulation : 5,41 cm, Gauche

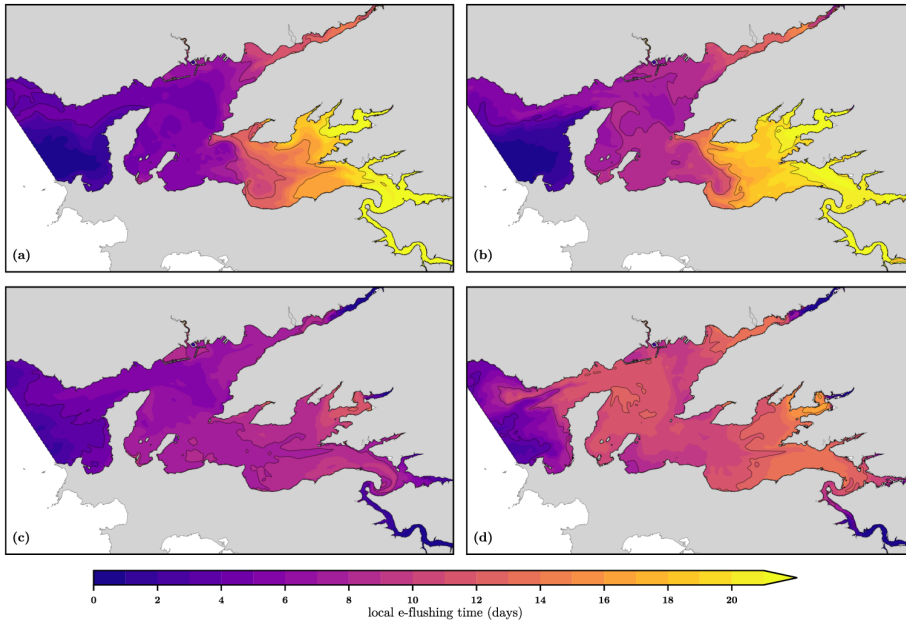


Figure 9: Local e-folding flushing time estimated for spring (a) and neap (b) tides in low-flow conditions and for spring (c) and neap (d) for flood conditions. Coastline source: SHOM.

2700

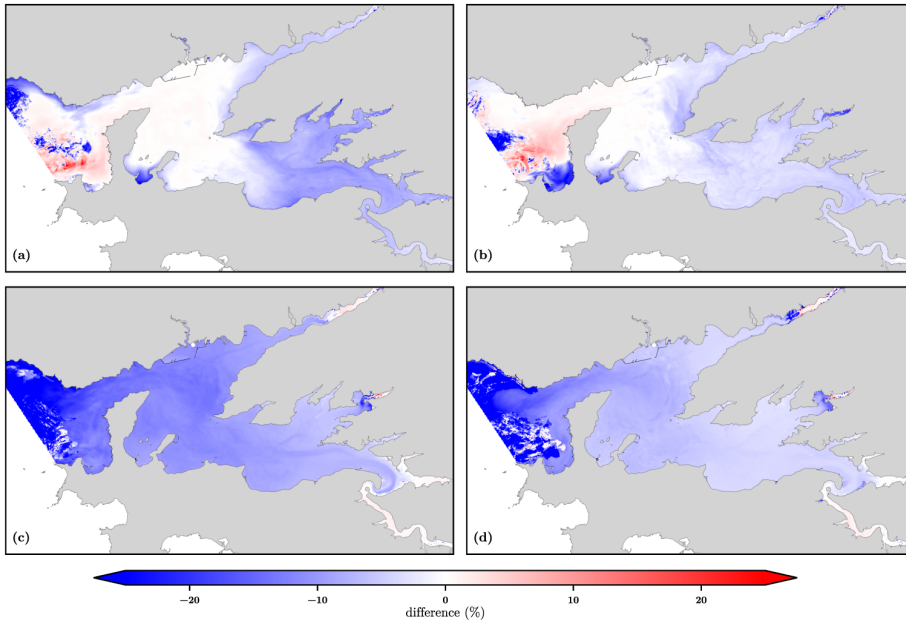


Figure 10: Differences between local e-folding flushing times estimated with one-way configuration over two-way nesting method. They are computed for spring (a) and neap (b) tides in low-flow conditions and for spring (c) and neap (d) for flood conditions. Coastline source: SHOM.

Page 2 : [1] a supprimé Sébastien Petton 24/01/2023 21:13:00

Page 2 : [1] a supprimé Sébastien Petton 24/01/2023 21:13:00

Page 2 : [1] a supprimé Sébastien Petton 24/01/2023 21:13:00

Page 2 : [1] a supprimé Sébastien Petton 24/01/2023 21:13:00

Page 2 : [1] a supprimé Sébastien Petton 24/01/2023 21:13:00

Page 2 : [1] a supprimé Sébastien Petton 24/01/2023 21:13:00

Page 2 : [1] a supprimé Sébastien Petton 24/01/2023 21:13:00

Page 2 : [1] a supprimé Sébastien Petton 24/01/2023 21:13:00

Page 2 : [1] a supprimé Sébastien Petton 24/01/2023 21:13:00

Page 2 : [1] a supprimé Sébastien Petton 24/01/2023 21:13:00

Page 2 : [2] a mis en forme Sébastien Petton 24/01/2023 21:13:00

Anglais (E.U.)

Page 2 : [2] a mis en forme Sébastien Petton 24/01/2023 21:13:00

Anglais (E.U.)

Page 2 : [3] a mis en forme Sébastien Petton 24/01/2023 21:13:00

Anglais (E.U.)

Page 2 : [3] a mis en forme Sébastien Petton 24/01/2023 21:13:00

Anglais (E.U.)

Page 2 : [4] a mis en forme Sébastien Petton 24/01/2023 21:13:00

Anglais (E.U.)

Page 2 : [4] a mis en forme Sébastien Petton 24/01/2023 21:13:00

Anglais (E.U.)

Page 2 : [6] a mis en forme Sébastien Petton 24/01/2023 21:13:00

Anglais (E.U.)

Page 2 : [6] a mis en forme Sébastien Petton 24/01/2023 21:13:00

Anglais (E.U.)

Page 2 : [7] a mis en forme Sébastien Petton 24/01/2023 21:13:00

Anglais (E.U.)

Page 2 : [7] a mis en forme Sébastien Petton 24/01/2023 21:13:00

Anglais (E.U.)

Page 2 : [8] a supprimé Sébastien Petton 24/01/2023 21:13:00

▼

Page 2 : [8] a supprimé Sébastien Petton 24/01/2023 21:13:00

▼

Page 2 : [9] a mis en forme Sébastien Petton 24/01/2023 21:13:00

Anglais (E.U.)

Page 2 : [9] a mis en forme Sébastien Petton 24/01/2023 21:13:00

Anglais (E.U.)

Page 2 : [10] a mis en forme Sébastien Petton 24/01/2023 21:13:00

Anglais (E.U.)

Page 2 : [10] a mis en forme Sébastien Petton 24/01/2023 21:13:00

Anglais (E.U.)

Page 2 : [11] a mis en forme Sébastien Petton 24/01/2023 21:13:00

Anglais (E.U.)

Page 2 : [11] a mis en forme Sébastien Petton 24/01/2023 21:13:00

Anglais (E.U.)

Page 2 : [12] a mis en forme Sébastien Petton 24/01/2023 21:13:00

Anglais (E.U.)

Page 2 : [12] a mis en forme Sébastien Petton 24/01/2023 21:13:00

Anglais (E.U.)

Page 2 : [13] a supprimé Sébastien Petton 24/01/2023 21:13:00

▼

Page 2 : [13] a supprimé Sébastien Petton 24/01/2023 21:13:00

▼

Page 2 : [14] a supprimé Sébastien Petton 24/01/2023 21:13:00



Page 2 : [14] a supprimé Sébastien Petton 24/01/2023 21:13:00



Page 2 : [14] a supprimé Sébastien Petton 24/01/2023 21:13:00



Page 3 : [15] a supprimé Sébastien Petton 24/01/2023 21:13:00



Page 3 : [15] a supprimé Sébastien Petton 24/01/2023 21:13:00



Page 3 : [15] a supprimé Sébastien Petton 24/01/2023 21:13:00



Page 3 : [15] a supprimé Sébastien Petton 24/01/2023 21:13:00



Page 3 : [15] a supprimé Sébastien Petton 24/01/2023 21:13:00



Page 3 : [15] a supprimé Sébastien Petton 24/01/2023 21:13:00



Page 3 : [15] a supprimé Sébastien Petton 24/01/2023 21:13:00



Page 3 : [15] a supprimé Sébastien Petton 24/01/2023 21:13:00



Page 3 : [15] a supprimé Sébastien Petton 24/01/2023 21:13:00



Page 3 : [15] a supprimé Sébastien Petton 24/01/2023 21:13:00



Page 3 : [15] a supprimé Sébastien Petton 24/01/2023 21:13:00



Page 3 : [15] a supprimé Sébastien Petton 24/01/2023 21:13:00



Page 3 : [15] a supprimé Sébastien Petton 24/01/2023 21:13:00



Page 3 : [16] a supprimé Sébastien Petton 24/01/2023 21:13:00



Page 3 : [16] a supprimé Sébastien Petton 24/01/2023 21:13:00



Page 3 : [16] a supprimé Sébastien Petton 24/01/2023 21:13:00



Page 3 : [16] a supprimé Sébastien Petton 24/01/2023 21:13:00



Page 3 : [17] a supprimé Sébastien Petton 24/01/2023 21:13:00



Page 3 : [17] a supprimé Sébastien Petton 24/01/2023 21:13:00



Page 3 : [17] a supprimé Sébastien Petton 24/01/2023 21:13:00



Page 3 : [17] a supprimé Sébastien Petton 24/01/2023 21:13:00



Page 3 : [17] a supprimé Sébastien Petton 24/01/2023 21:13:00



Page 3 : [17] a supprimé Sébastien Petton 24/01/2023 21:13:00



Page 3 : [17] a supprimé Sébastien Petton 24/01/2023 21:13:00



Page 3 : [18] a supprimé Sébastien Petton 24/01/2023 21:13:00



Page 3 : [18] a supprimé Sébastien Petton 24/01/2023 21:13:00



Page 3 : [19] a supprimé Sébastien Petton 24/01/2023 21:13:00



Page 3 : [19] a supprimé Sébastien Petton 24/01/2023 21:13:00



Page 4 : [20] a supprimé Sébastien Petton 24/01/2023 21:13:00



Page 4 : [21] a supprimé Sébastien Petton 24/01/2023 21:13:00



Page 4 : [21] a supprimé Sébastien Petton 24/01/2023 21:13:00



Page 4 : [22] a supprimé Sébastien Petton 24/01/2023 21:13:00



Page 4 : [22] a supprimé Sébastien Petton 24/01/2023 21:13:00



Page 4 : [22] a supprimé Sébastien Petton 24/01/2023 21:13:00



Page 4 : [22] a supprimé Sébastien Petton 24/01/2023 21:13:00



Page 4 : [22] a supprimé Sébastien Petton 24/01/2023 21:13:00



Page 4 : [22] a supprimé Sébastien Petton 24/01/2023 21:13:00



Page 4 : [23] a supprimé Sébastien Petton 24/01/2023 21:13:00



Page 4 : [23] a supprimé Sébastien Petton 24/01/2023 21:13:00



Page 4 : [24] a supprimé Sébastien Petton 24/01/2023 21:13:00



Page 4 : [24] a supprimé Sébastien Petton 24/01/2023 21:13:00



Page 4 : [24] a supprimé Sébastien Petton 24/01/2023 21:13:00



Page 4 : [24] a supprimé Sébastien Petton 24/01/2023 21:13:00



Page 4 : [25] a supprimé Sébastien Petton 24/01/2023 21:13:00



Page 4 : [25] a supprimé Sébastien Petton 24/01/2023 21:13:00



Page 4 : [27] a supprimé Sébastien Petton 24/01/2023 21:13:00



Page 4 : [27] a supprimé Sébastien Petton 24/01/2023 21:13:00



Page 4 : [27] a supprimé Sébastien Petton 24/01/2023 21:13:00



Page 4 : [27] a supprimé Sébastien Petton 24/01/2023 21:13:00



Page 4 : [27] a supprimé Sébastien Petton 24/01/2023 21:13:00



Page 4 : [27] a supprimé Sébastien Petton 24/01/2023 21:13:00



Page 4 : [27] a supprimé Sébastien Petton 24/01/2023 21:13:00



Page 4 : [27] a supprimé Sébastien Petton 24/01/2023 21:13:00



Page 4 : [28] a supprimé Sébastien Petton 24/01/2023 21:13:00



Page 4 : [28] a supprimé Sébastien Petton 24/01/2023 21:13:00



Page 4 : [28] a supprimé Sébastien Petton 24/01/2023 21:13:00



Page 4 : [28] a supprimé Sébastien Petton 24/01/2023 21:13:00



Page 4 : [28] a supprimé Sébastien Petton 24/01/2023 21:13:00



Page 4 : [28] a supprimé Sébastien Petton 24/01/2023 21:13:00



Page 5 : [29] a supprimé Sébastien Petton 24/01/2023 21:13:00



Page 5 : [29] a supprimé Sébastien Petton 24/01/2023 21:13:00



Page 5 : [30] a mis en forme Sébastien Petton 24/01/2023 21:13:00

Anglais (E.U.)

Page 5 : [31] a supprimé Sébastien Petton 24/01/2023 21:13:00

▼

Page 5 : [31] a supprimé Sébastien Petton 24/01/2023 21:13:00

▼

Page 5 : [31] a supprimé Sébastien Petton 24/01/2023 21:13:00

▼

Page 5 : [31] a supprimé Sébastien Petton 24/01/2023 21:13:00

▼

Page 5 : [31] a supprimé Sébastien Petton 24/01/2023 21:13:00

▼

Page 5 : [32] a mis en forme Sébastien Petton 24/01/2023 21:13:00

Anglais (E.U.)

Page 5 : [32] a mis en forme Sébastien Petton 24/01/2023 21:13:00

Anglais (E.U.)

Page 5 : [32] a mis en forme Sébastien Petton 24/01/2023 21:13:00

Anglais (E.U.)

Page 5 : [33] a supprimé Sébastien Petton 24/01/2023 21:13:00

▼

Page 5 : [33] a supprimé Sébastien Petton 24/01/2023 21:13:00

▼

Page 5 : [34] a mis en forme Sébastien Petton 24/01/2023 21:13:00

Anglais (E.U.)

Page 5 : [34] a mis en forme Sébastien Petton 24/01/2023 21:13:00

Anglais (E.U.)

Page 5 : [35] a supprimé Sébastien Petton 24/01/2023 21:13:00

▼

Page 5 : [35] a supprimé Sébastien Petton 24/01/2023 21:13:00

▼

Page 5 : [35] a supprimé Sébastien Petton 24/01/2023 21:13:00

▼

Page 5 : [37] a supprimé Sébastien Petton 24/01/2023 21:13:00



Page 5 : [37] a supprimé Sébastien Petton 24/01/2023 21:13:00



Page 5 : [37] a supprimé Sébastien Petton 24/01/2023 21:13:00



Page 5 : [38] a supprimé Sébastien Petton 24/01/2023 21:13:00



Page 5 : [38] a supprimé Sébastien Petton 24/01/2023 21:13:00



Page 5 : [38] a supprimé Sébastien Petton 24/01/2023 21:13:00



Page 5 : [38] a supprimé Sébastien Petton 24/01/2023 21:13:00



Page 5 : [38] a supprimé Sébastien Petton 24/01/2023 21:13:00



Page 5 : [38] a supprimé Sébastien Petton 24/01/2023 21:13:00



Page 5 : [38] a supprimé Sébastien Petton 24/01/2023 21:13:00



Page 5 : [39] a supprimé Sébastien Petton 24/01/2023 21:13:00



Page 5 : [39] a supprimé Sébastien Petton 24/01/2023 21:13:00



Page 5 : [39] a supprimé Sébastien Petton 24/01/2023 21:13:00



Page 5 : [39] a supprimé Sébastien Petton 24/01/2023 21:13:00



Page 8 : [40] a supprimé Sébastien Petton 24/01/2023 21:13:00



Page 8 : [41] a supprimé Sébastien Petton 24/01/2023 21:13:00



Page 9 : [43] a supprimé Sébastien Petton 24/01/2023 21:13:00



Page 9 : [43] a supprimé Sébastien Petton 24/01/2023 21:13:00



Page 9 : [43] a supprimé Sébastien Petton 24/01/2023 21:13:00



Page 9 : [44] a supprimé Sébastien Petton 24/01/2023 21:13:00



Page 9 : [44] a supprimé Sébastien Petton 24/01/2023 21:13:00



Page 9 : [44] a supprimé Sébastien Petton 24/01/2023 21:13:00



Page 9 : [44] a supprimé Sébastien Petton 24/01/2023 21:13:00



Page 9 : [44] a supprimé Sébastien Petton 24/01/2023 21:13:00



Page 9 : [44] a supprimé Sébastien Petton 24/01/2023 21:13:00



Page 9 : [44] a supprimé Sébastien Petton 24/01/2023 21:13:00



Page 9 : [44] a supprimé Sébastien Petton 24/01/2023 21:13:00



Page 9 : [44] a supprimé Sébastien Petton 24/01/2023 21:13:00



Page 9 : [44] a supprimé Sébastien Petton 24/01/2023 21:13:00



Page 9 : [44] a supprimé Sébastien Petton 24/01/2023 21:13:00



Page 9 : [44] a supprimé Sébastien Petton 24/01/2023 21:13:00



Page 9 : [44] a supprimé Sébastien Petton 24/01/2023 21:13:00



Page 9 : [44] a supprimé Sébastien Petton 24/01/2023 21:13:00



Page 9 : [45] a supprimé Sébastien Petton 24/01/2023 21:13:00



Page 9 : [45] a supprimé Sébastien Petton 24/01/2023 21:13:00



Page 9 : [45] a supprimé Sébastien Petton 24/01/2023 21:13:00



Page 9 : [45] a supprimé Sébastien Petton 24/01/2023 21:13:00



Page 9 : [45] a supprimé Sébastien Petton 24/01/2023 21:13:00



Page 9 : [45] a supprimé Sébastien Petton 24/01/2023 21:13:00



Page 9 : [45] a supprimé Sébastien Petton 24/01/2023 21:13:00



Page 9 : [45] a supprimé Sébastien Petton 24/01/2023 21:13:00



Page 9 : [46] a supprimé Sébastien Petton 24/01/2023 21:13:00



Page 9 : [46] a supprimé Sébastien Petton 24/01/2023 21:13:00



Page 9 : [46] a supprimé Sébastien Petton 24/01/2023 21:13:00



Page 9 : [46] a supprimé Sébastien Petton 24/01/2023 21:13:00



Page 9 : [46] a supprimé Sébastien Petton 24/01/2023 21:13:00



Page 9 : [46] a supprimé Sébastien Petton 24/01/2023 21:13:00



Page 9 : [46] a supprimé Sébastien Petton 24/01/2023 21:13:00



Page 9 : [46] a supprimé Sébastien Petton 24/01/2023 21:13:00



Page 9 : [46] a supprimé Sébastien Petton 24/01/2023 21:13:00



Page 9 : [46] a supprimé Sébastien Petton 24/01/2023 21:13:00



Page 9 : [46] a supprimé Sébastien Petton 24/01/2023 21:13:00



Page 10 : [47] a supprimé Sébastien Petton 24/01/2023 21:13:00



Page 10 : [48] a mis en forme Sébastien Petton 24/01/2023 21:13:00

Anglais (E.U.)

Page 10 : [49] a mis en forme Sébastien Petton 24/01/2023 21:13:00

Anglais (E.U.)

Page 10 : [50] a supprimé Sébastien Petton 24/01/2023 21:13:00



Page 10 : [51] a supprimé Sébastien Petton 24/01/2023 21:13:00



Page 10 : [52] a supprimé Sébastien Petton 24/01/2023 21:13:00



Page 12 : [53] a supprimé Sébastien Petton 24/01/2023 21:13:00



Page 14 : [54] a mis en forme Sébastien Petton 24/01/2023 21:13:00

Anglais (E.U.)

Page 14 : [54] a mis en forme Sébastien Petton 24/01/2023 21:13:00

Anglais (E.U.)

Page 14 : [55] a supprimé Sébastien Petton 24/01/2023 21:13:00



Page 14 : [55] a supprimé Sébastien Petton 24/01/2023 21:13:00



Page 14 : [56] a mis en forme Sébastien Petton 24/01/2023 21:13:00

Anglais (E.U.)

Page 14 : [57] a supprimé **Sébastien Petton** **24/01/2023 21:13:00**



Page 14 : [57] a supprimé **Sébastien Petton** **24/01/2023 21:13:00**



Page 14 : [57] a supprimé **Sébastien Petton** **24/01/2023 21:13:00**



Page 14 : [57] a supprimé **Sébastien Petton** **24/01/2023 21:13:00**



Page 14 : [58] a supprimé **Sébastien Petton** **24/01/2023 21:13:00**



Page 14 : [58] a supprimé **Sébastien Petton** **24/01/2023 21:13:00**



Page 14 : [58] a supprimé **Sébastien Petton** **24/01/2023 21:13:00**



Page 14 : [58] a supprimé **Sébastien Petton** **24/01/2023 21:13:00**



Page 14 : [59] a supprimé **Sébastien Petton** **24/01/2023 21:13:00**



Page 14 : [59] a supprimé **Sébastien Petton** **24/01/2023 21:13:00**



Page 14 : [59] a supprimé **Sébastien Petton** **24/01/2023 21:13:00**



Page 14 : [60] a supprimé **Sébastien Petton** **24/01/2023 21:13:00**



Page 14 : [60] a supprimé **Sébastien Petton** **24/01/2023 21:13:00**



Page 14 : [60] a supprimé **Sébastien Petton** **24/01/2023 21:13:00**



Page 14 : [60] a supprimé **Sébastien Petton** **24/01/2023 21:13:00**



Page 14 : [60] a supprimé **Sébastien Petton** **24/01/2023 21:13:00**



Page 14 : [62] a supprimé **Sébastien Petton** **24/01/2023 21:13:00**

▼

Page 14 : [62] a supprimé **Sébastien Petton** **24/01/2023 21:13:00**

▼

Page 14 : [63] a mis en forme **Sébastien Petton** **24/01/2023 21:13:00**

Anglais (E.U.)

Page 14 : [63] a mis en forme **Sébastien Petton** **24/01/2023 21:13:00**

Anglais (E.U.)

Page 14 : [64] a supprimé **Sébastien Petton** **24/01/2023 21:13:00**

▼

Page 14 : [64] a supprimé **Sébastien Petton** **24/01/2023 21:13:00**

▼

Page 14 : [64] a supprimé **Sébastien Petton** **24/01/2023 21:13:00**

▼

Page 14 : [64] a supprimé **Sébastien Petton** **24/01/2023 21:13:00**

▼

Page 14 : [64] a supprimé **Sébastien Petton** **24/01/2023 21:13:00**

▼

Page 14 : [64] a supprimé **Sébastien Petton** **24/01/2023 21:13:00**

▼

Page 14 : [64] a supprimé **Sébastien Petton** **24/01/2023 21:13:00**

▼

Page 14 : [64] a supprimé **Sébastien Petton** **24/01/2023 21:13:00**

▼

Page 14 : [64] a supprimé **Sébastien Petton** **24/01/2023 21:13:00**

▼

Page 14 : [64] a supprimé **Sébastien Petton** **24/01/2023 21:13:00**

▼

Page 14 : [64] a supprimé **Sébastien Petton** **24/01/2023 21:13:00**

▼

Page 14 : [65] a supprimé **Sébastien Petton** **24/01/2023 21:13:00**

▼

Page 14 : [65] a supprimé Sébastien Petton 24/01/2023 21:13:00

▼

Page 14 : [66] a mis en forme Sébastien Petton 24/01/2023 21:13:00

Anglais (E.U.)

Page 14 : [66] a mis en forme Sébastien Petton 24/01/2023 21:13:00

Anglais (E.U.)

Page 14 : [67] a mis en forme Sébastien Petton 24/01/2023 21:13:00

Anglais (E.U.)

Page 14 : [67] a mis en forme Sébastien Petton 24/01/2023 21:13:00

Anglais (E.U.)

Page 14 : [68] a mis en forme Sébastien Petton 24/01/2023 21:13:00

Anglais (E.U.)

Page 14 : [68] a mis en forme Sébastien Petton 24/01/2023 21:13:00

Anglais (E.U.)

Page 14 : [69] a mis en forme Sébastien Petton 24/01/2023 21:13:00

Anglais (E.U.)

Page 14 : [69] a mis en forme Sébastien Petton 24/01/2023 21:13:00

Anglais (E.U.)

Page 15 : [70] a supprimé Sébastien Petton 24/01/2023 21:13:00

▼

Page 15 : [71] a supprimé Sébastien Petton 24/01/2023 21:13:00

▼

Page 15 : [72] a supprimé Sébastien Petton 24/01/2023 21:13:00

▼

Page 15 : [73] a supprimé Sébastien Petton 24/01/2023 21:13:00

▼

Page 15 : [74] a supprimé Sébastien Petton 24/01/2023 21:13:00

▼

Page 16 : [75] a supprimé Sébastien Petton 24/01/2023 21:13:00

▼

Page 16 : [76] a supprimé Sébastien Petton 24/01/2023 21:13:00

▼

Page 16 : [77] a supprimé Sébastien Petton 24/01/2023 21:13:00

▼
Page 17 : [79] a supprimé Sébastien Petton 24/01/2023 21:13:00

▼
Page 17 : [79] a supprimé Sébastien Petton 24/01/2023 21:13:00

▼
Page 17 : [79] a supprimé Sébastien Petton 24/01/2023 21:13:00

▼
Page 17 : [79] a supprimé Sébastien Petton 24/01/2023 21:13:00

▼
Page 17 : [80] a supprimé Sébastien Petton 24/01/2023 21:13:00

▼
Page 17 : [80] a supprimé Sébastien Petton 24/01/2023 21:13:00

▼
Page 17 : [80] a supprimé Sébastien Petton 24/01/2023 21:13:00

▼
Page 17 : [80] a supprimé Sébastien Petton 24/01/2023 21:13:00

▼
Page 17 : [80] a supprimé Sébastien Petton 24/01/2023 21:13:00

▼
Page 17 : [80] a supprimé Sébastien Petton 24/01/2023 21:13:00

▼
Page 17 : [80] a supprimé Sébastien Petton 24/01/2023 21:13:00

▼
Page 17 : [80] a supprimé Sébastien Petton 24/01/2023 21:13:00

▼
Page 17 : [80] a supprimé Sébastien Petton 24/01/2023 21:13:00

▼
Page 17 : [80] a supprimé Sébastien Petton 24/01/2023 21:13:00

▼
Page 17 : [80] a supprimé Sébastien Petton 24/01/2023 21:13:00

▼
Page 17 : [80] a supprimé Sébastien Petton 24/01/2023 21:13:00

▼
Page 17 : [80] a supprimé Sébastien Petton 24/01/2023 21:13:00

▼
Page 17 : [81] a supprimé Sébastien Petton 24/01/2023 21:13:00

▼
Page 17 : [81] a supprimé Sébastien Petton 24/01/2023 21:13:00

▼
Page 17 : [82] a mis en forme Sébastien Petton 24/01/2023 21:13:00
Anglais (E.U.)

▼
Page 17 : [82] a mis en forme Sébastien Petton 24/01/2023 21:13:00
Anglais (E.U.)

▼
Page 17 : [83] a supprimé Sébastien Petton 24/01/2023 21:13:00

▼
Page 17 : [83] a supprimé Sébastien Petton 24/01/2023 21:13:00

▼
Page 17 : [83] a supprimé Sébastien Petton 24/01/2023 21:13:00

▼
Page 17 : [83] a supprimé Sébastien Petton 24/01/2023 21:13:00

▼
Page 17 : [83] a supprimé Sébastien Petton 24/01/2023 21:13:00

▼
Page 17 : [83] a supprimé Sébastien Petton 24/01/2023 21:13:00

▼
Page 17 : [83] a supprimé Sébastien Petton 24/01/2023 21:13:00

▼
Page 17 : [83] a supprimé Sébastien Petton 24/01/2023 21:13:00

▼
Page 17 : [83] a supprimé Sébastien Petton 24/01/2023 21:13:00

▼
Page 17 : [84] a supprimé Sébastien Petton 24/01/2023 21:13:00

▼
Page 17 : [84] a supprimé Sébastien Petton 24/01/2023 21:13:00

▼
Page 17 : [84] a supprimé Sébastien Petton 24/01/2023 21:13:00

▼
Page 17 : [85] a supprimé Sébastien Petton 24/01/2023 21:13:00

▼
Page 17 : [85] a supprimé Sébastien Petton 24/01/2023 21:13:00

▼
Page 17 : [85] a supprimé Sébastien Petton 24/01/2023 21:13:00

▼
Page 17 : [85] a supprimé Sébastien Petton 24/01/2023 21:13:00

▼
Page 18 : [86] a supprimé Sébastien Petton 24/01/2023 21:13:00

▼
Page 18 : [86] a supprimé Sébastien Petton 24/01/2023 21:13:00

▼
Page 18 : [86] a supprimé Sébastien Petton 24/01/2023 21:13:00

▼
Page 18 : [86] a supprimé Sébastien Petton 24/01/2023 21:13:00

▼
Page 18 : [87] a supprimé Sébastien Petton 24/01/2023 21:13:00

▼
Page 18 : [87] a supprimé Sébastien Petton 24/01/2023 21:13:00

▼
Page 18 : [87] a supprimé Sébastien Petton 24/01/2023 21:13:00

▼
Page 18 : [87] a supprimé Sébastien Petton 24/01/2023 21:13:00

▼
Page 18 : [87] a supprimé Sébastien Petton 24/01/2023 21:13:00

▼
Page 18 : [87] a supprimé Sébastien Petton 24/01/2023 21:13:00

▼
Page 18 : [87] a supprimé Sébastien Petton 24/01/2023 21:13:00

Anglais (E.U.)

Page 18 : [89] a supprimé Sébastien Petton 24/01/2023 21:13:00



Page 18 : [89] a supprimé Sébastien Petton 24/01/2023 21:13:00



Page 18 : [89] a supprimé Sébastien Petton 24/01/2023 21:13:00



Page 18 : [89] a supprimé Sébastien Petton 24/01/2023 21:13:00



Page 18 : [90] a supprimé Sébastien Petton 24/01/2023 21:13:00



Page 18 : [90] a supprimé Sébastien Petton 24/01/2023 21:13:00



Page 18 : [90] a supprimé Sébastien Petton 24/01/2023 21:13:00



Page 18 : [90] a supprimé Sébastien Petton 24/01/2023 21:13:00



Page 18 : [90] a supprimé Sébastien Petton 24/01/2023 21:13:00



Page 18 : [90] a supprimé Sébastien Petton 24/01/2023 21:13:00



Page 18 : [90] a supprimé Sébastien Petton 24/01/2023 21:13:00



Page 18 : [91] a supprimé Sébastien Petton 24/01/2023 21:13:00



Page 18 : [91] a supprimé Sébastien Petton 24/01/2023 21:13:00



Page 18 : [91] a supprimé Sébastien Petton 24/01/2023 21:13:00



Page 18 : [92] a supprimé Sébastien Petton 24/01/2023 21:13:00



Page 18 : [92] a supprimé Sébastien Petton 24/01/2023 21:13:00

▼
Page 18 : [92] a supprimé Sébastien Petton 24/01/2023 21:13:00

▼
Page 18 : [92] a supprimé Sébastien Petton 24/01/2023 21:13:00

▼
Page 18 : [92] a supprimé Sébastien Petton 24/01/2023 21:13:00

▼
Page 18 : [92] a supprimé Sébastien Petton 24/01/2023 21:13:00

▼
Page 18 : [92] a supprimé Sébastien Petton 24/01/2023 21:13:00

▼
Page 18 : [92] a supprimé Sébastien Petton 24/01/2023 21:13:00

▼
Page 18 : [92] a supprimé Sébastien Petton 24/01/2023 21:13:00

▼
Page 18 : [93] a supprimé Sébastien Petton 24/01/2023 21:13:00

▼
Page 18 : [93] a supprimé Sébastien Petton 24/01/2023 21:13:00

▼
Page 18 : [93] a supprimé Sébastien Petton 24/01/2023 21:13:00

▼
Page 18 : [93] a supprimé Sébastien Petton 24/01/2023 21:13:00

▼
Page 18 : [94] a supprimé Sébastien Petton 24/01/2023 21:13:00

▼
Page 18 : [94] a supprimé Sébastien Petton 24/01/2023 21:13:00

▼
Page 18 : [94] a supprimé Sébastien Petton 24/01/2023 21:13:00

▼
Page 18 : [94] a supprimé Sébastien Petton 24/01/2023 21:13:00

▼
Page 18 : [94] a supprimé Sébastien Petton 24/01/2023 21:13:00

▼.....
Page 19 : [95] a supprimé Sébastien Petton 24/01/2023 21:13:00

▼.....
Page 19 : [96] a mis en forme Sébastien Petton 24/01/2023 21:13:00

Police :Gras, Couleur de police : Noir, Non Barré, Crenage 16 pt

▼.....
Page 19 : [97] a supprimé Sébastien Petton 24/01/2023 21:13:00

▼.....
Page 19 : [98] a supprimé Sébastien Petton 24/01/2023 21:13:00

▼.....
Page 19 : [99] a mis en forme Sébastien Petton 24/01/2023 21:13:00

Police :Gras, Couleur de police : Noir, Non Barré, Crenage 16 pt